



## An algorithm to retrieve chlorophyll, dissolved organic carbon, and suspended minerals from Great Lakes satellite data



Robert A. Shuchman <sup>a,\*</sup>, George Leshkevich <sup>b,1</sup>, Michael J. Sayers <sup>a,2</sup>, Thomas H. Johengen <sup>c,3</sup>, Colin N. Brooks <sup>a,4</sup>, Dmitry Pozdnyakov <sup>d,5</sup>

<sup>a</sup> Michigan Tech Research Institute (MTRI), Michigan Technological University, 3600 Green Ct., Ste 100, Ann Arbor, MI 48105, USA

<sup>b</sup> National Oceanic and Atmospheric Administration (NOAA)/Great Lakes Environmental Research Laboratory (GLERL), 4840 S. State Rd, Ann Arbor, MI 48108, USA

<sup>c</sup> Cooperative Institute for Limnology and Ecosystems Research (CILER), University of Michigan, 4840 S. State Rd, Ann Arbor, MI 48108, USA

<sup>d</sup> Nansen International Environmental and Remote Sensing Centre (NIERSC), 7, 14th Line, office 49, Business Centre "Preobrazhensky", Vasilievsky Island, 199034 St. Petersburg, Russia

### ARTICLE INFO

#### Article history:

Received 26 January 2012

Accepted 28 April 2013

Available online 4 August 2013

Communicated by Barry Lesht

#### Keywords:

Chlorophyll  
Remote sensing  
Great Lakes  
MODIS, MERIS  
SeaWiFS  
Water color

### ABSTRACT

An algorithm that utilizes individual lake hydro-optical (HO) models has been developed for the Great Lakes that uses SeaWiFS, MODIS, or MERIS satellite data to estimate concentrations of chlorophyll, dissolved organic carbon, and suspended minerals. The Color Producing Agent Algorithm (CPA-A) uses a specific HO model for each lake. The HO models provide absorption functions for the Color Producing Agents (CPAs) (chlorophyll (chl), colored dissolved organic matter (as dissolved organic carbon, doc), and suspended minerals (sm)) as well as backscatter for the chlorophyll, and suspended mineral parameters. These models were generated using simultaneous optical data collected with in situ measurements of CPAs collected during research cruises in the Great Lakes using regression analysis as well as using specific absorption and backscatter coefficients at specific chl, doc, and sm concentrations. A single average HO model for the Great Lakes was found to generate insufficiently accurate concentrations for Lakes Michigan, Erie, Superior and Huron. These new individual lake retrievals were evaluated with respect to EPA in situ field observations, as well as compared to the widely used OC3 MODIS retrieval. The new algorithm retrievals provided slightly more accurate chl values for Lakes Michigan, Superior, Huron, and Ontario than those obtained using the OC3 approach as well as providing additional concentration information on doc and sm. The CPA-A chl retrieval for Lake Erie is quite robust, producing reliable chl values in the reported EPA concentration ranges. Atmospheric correction approaches were also evaluated in this study.

© 2013 International Association for Great Lakes Research. Published by Elsevier B.V. All rights reserved.

### Introduction

Satellite remote sensing of the Great Lakes has become increasingly important over the past two decades. The Great Lakes account for approximately 20% of the Earth's surface fresh water and supplies drinking water for forty million United States and Canadian people (Van der Leeden et al., 1991). Lakes Michigan and Huron in particular have undergone major changes in lower food web production as witnessed by decreases in average chlorophyll, primary productivity, *Diporeia*, and fish populations (Fahnenstiel et al., 2010a,b; Nalepa et al., 2009). Lake Erie and to a lesser extent Lake Ontario continue to exhibit multiple

Harmful Algal Blooms (HABs) each summer (Boyer, 2008; Rinta-Kanto et al., 2005). Remote sensing observations from satellites allow for the synoptic long term monitoring of all the Laurentian Great Lakes to document changes in water quality parameters and primary productivity as a result of the climate, anthropogenic, and invasive species forcing functions.

Only visible radiation penetrates into a water column to any great extent (Jerlov, 1976). As light travels through the water column it interacts with both molecules and particles that comprise the chlorophyll (chl), colored dissolved organic matter (cdom) and inorganic suspended minerals (sm) resulting in alterations of the upwelling radiative flux (Pozdnyakov and Grassel, 2003). Thus the backscattered flux emerging from beneath the water surface contains information about the optical properties of the water column which when observed over time provides insight into the dynamic processes of the Great Lakes (Shuchman et al., 2006).

For the open ocean case, the satellite retrieval of the chlorophyll and other related water quality parameters is straight forward. For example the OC3, OC4 and other algorithms currently used by NASA for the open ocean (Ackleson, 2001; O'Reilly et al., 1998, 2000a) are empirical, visible (blue/green) band ratio techniques. These algorithms are effective due

\* Corresponding author. Tel.: +1 734 913 6860.

E-mail addresses: [shuchman@mtu.edu](mailto:shuchman@mtu.edu) (R.A. Shuchman), [george.leshkevich@noaa.gov](mailto:george.leshkevich@noaa.gov) (G. Leshkevich), [mjsayers@mtu.edu](mailto:mjsayers@mtu.edu) (M.J. Sayers), [tom.johengen@noaa.gov](mailto:tom.johengen@noaa.gov) (T.H. Johengen), [colin.brooks@mtu.edu](mailto:colin.brooks@mtu.edu) (C.N. Brooks), [dmitry.pozdnyakov@niersc.spb.ru](mailto:dmitry.pozdnyakov@niersc.spb.ru) (D. Pozdnyakov).

<sup>1</sup> Tel.: +1 734 741 2265; fax: +1 734 741 2055.

<sup>2</sup> Tel.: +1 734 913 6852.

<sup>3</sup> Tel.: +1 734 741 2203; fax: +1 734 741 2055.

<sup>4</sup> Tel.: +1 734 913 6858; fax: +1 734 913 6880.

<sup>5</sup> Tel.: +7 812 324 51 03; fax: +7 812 324 51 02.

to the optical simplicity of the ocean water which is dominated by indigenous phytoplankton and are referred to as Case I waters by Morel and Prieur (1977).

Some waters in the Great Lakes and coastal ocean areas, known as the Morel and Prieur Case II waters, have optical properties that are influenced not only by phytoplankton, but also by inorganic terrigenous particulate matter in suspension (sm) and the colored portion of dissolved organic carbon (doc). In some areas of the Great Lakes and in particular the near shore, bays, river mouths, and areas of concern (AOCs) the content of sm and doc in the water column is abundant enough to compete with the phytoplankton in influencing the resultant composite optical properties, thus creating optically complex water (Bukata et al., 1985; Mortimer, 1988). It is this complexity that impacts the performance of ocean based ratio techniques.

Recent attempts to generate optical algorithms to retrieve chlorophyll concentrations in complex Great Lakes waters are also producing promising results. Binding et al. (2012) have constructed a model that uses both red and near-infrared wavelengths to retrieve both concentrations of chlorophyll and suspended sediments in Lake Erie. This model is unaffected by the presence of cdom which is not only detected in the blue wavelengths but is also sensitive to suspended sediment reflectance in the red wavelengths. Lesht et al. (2013) have modified the blue-green band ratio technique created for use in the open ocean by generating sensor specific coefficients from near simultaneous satellite and field data sets that produce good chlorophyll estimates in the offshore “open” portions of the Great Lakes. While these algorithms show great potential in certain portions of the Great Lakes, a full spectrum algorithm, like the CPA-A, with robust water optical characterization can be implemented for all types of Great Lakes water.

When observing Case II waters from space over the full visible electromagnetic spectrum, it is impractical to retrieve the concentration of a single component like chl without also inferring the content of the other major water constituents determining the overall color, the so called color producing agents (CPAs) (Pozdnyakov et al., 2005). Bukata et al. (1995) determined through simultaneous optical and in situ measurements on Lake Ontario that in the Great Lakes the other two CPAs in addition to chl are cdom and sm. A principal component analysis reported by Shuchman et al. (2006) further confirmed Bukata supposition that chl, cdom, and sm generate the color of the Great lakes observed from space.

Thus, in summary, water color in inland and coastal water results mainly from three different parameters, referred to as CPAs. They include: 1) chlorophyll, chromophoric dissolved organic matter and suspended minerals. Chlorophyll (chl) is the green pigment found in plant cells that are suspended in the water and produce a green-yellow color. Chl not only absorbs light but also contributes to the overall water light scattering through complex interactions as well (Bukata et al., 1995). Dissolved organic carbon is a product micro-organism metabolism and can be produced in situ in the lake or transported from decaying vegetation via rivers and streams. The cdom portion of the doc both absorbs and scatters light, however due to a small number of doc molecules per unit volume compared to the number of water molecules in this unit volume, the cdom contribution to molecular scattering is believed to be negligible (no backscatter component). Suspended minerals (sm) constitute inorganic particles that can both scatter and absorb light.

The Color Producing Agent Algorithm (CPA-A) presented here uses a Levenberg–Marquardt (L-M) multivariate optimization procedure (Levenberg, 1944; Marquardt, 1963) to estimate chl, cdom, and sm based on hydro-optical (HO) models. These HO models were generated using simultaneous near surface optical data collected with in situ water chemistry measurements of the three primary components collected during research cruises in all the Great lakes using multiple regression analysis as well as using specific absorption and backscatter coefficients at specific chl, doc, and sm concentrations. The algorithm is non-satellite specific and the number of spectral bands used is

variable depending on application. The algorithm identifies and discards pixels with poor atmospheric correction and/or water optical properties incompatible with the applied HO models. Pixels in optically shallow water (reflected light from the lake bottom) are also discarded during the retrieval process. Unlike the original algorithm used in the previous Lake Michigan Study (Shuchman et al., 2006) the CPA-A algorithm does not use neural net techniques for generation of the initial starting point of the retrieval process.

The cdom reflectance signature recorded from satellite observations is inverted to a doc concentration estimate via the HO model to provide a more meaningful water quality parameter to the user and also to be consistent with the chl and sm concentrations, rather than retrieved band specific cdom absorption. The methodology to derive doc from cdom is discussed in the [Hydro-optical model generation and algorithm description](#) section of the paper. Hence throughout this paper doc is presented as one of the three outputs of the CPA-A, but it should be noted that cdom is the constituent actually contributing to the satellite measured water reflectance signature.

Atmospheric correction of satellite data is a very important factor in determining the accuracy of the CPA-A estimates (Land and Haigh, 1997; Ruddick et al., 2000). The challenge over Case II waters is obtaining a highly precise assessment of the path radiance originating from photon interactions with atmospheric aerosols, particularly in the lower troposphere. In Case I waters, typically offshore, the atmospheric aerosols are generally homogeneous throughout the optical path length, dominated by scattering from the aerosols and can be adequately corrected to within 5% (Pozdnyakov et al., 2000a). Because they are generally located near shore or in waters closely bounded by land, the aerosols found over Case II waters are more likely to be influenced by varied continental sources and are no longer uniformly distributed and include both scattering and absorption components. The aerosols come from a number of point and distributed sources often anthropogenic in nature. Atmospheric aerosol correction models that rely on the Near Infrared (NIR) black pixel assumption (Gordon and Clark, 1981) also can fail in some Case II waters where sufficient quantities of CPAs can reflect enough NIR light to violate this assumption. Case II atmospheric correction error, with respect to corrected satellite observed reflectance compared to in situ spectra, can be as high as 15% which can adversely affect the performance of the retrieval algorithms (Pozdnyakov et al., 2000b). Thus, an aspect of this study was to evaluate the recommended suite of atmospheric corrections available to MODIS data users on three Great Lakes data sets where coincident ship based radiometer data was available.

A number of investigators (Budd and Warrington, 2004; Kerfoot et al., 2008; Lesht et al., 2012; Stumpf, 2001) have used OC3 retrievals of chl for Great Lakes investigations with success. These studies which included some limited comparisons with field campaigns show in general that chl retrieval in the open/offshore portions (optically deep) of Lakes Michigan, Huron, Superior and portions of Ontario where the color component observed is dominated by chl can be used to generate meaningful time series. However, Bergmann et al. found that in Lake Michigan there were statistically significant deviations between in situ measured and OC3 modeled chlorophyll concentrations when cryptophytes make up a large percentage (>40%) of the total chlorophyll (Bergmann et al., 2004) indicating potential limitations of ratio based methods to produce accurate chlorophyll retrievals in dynamic phytoplankton regimes. In areas of the Great lakes such as the near shore and bays where the observed color is a result of chl, cdom and sm the OC3 retrieval values are overestimated, a consequence of the band ratio approach assuming a single CPA component, namely phytoplankton (Lohrenz et al., 2008). The high shallow water chl concentrations provided by the OC3 blue-green band ratio technique in the near shore are also exacerbated by reflection off the lake bottom in optically shallow water (D'Sa et al., 2002; Lee et al., 2001). Comparison of standard OC3 retrievals in Lakes Erie and the western basin of Ontario does not consistently compare well with in situ observations (Witter et al., 2009) again due to the fact that all

of Lake Erie and a significant portion of Lake Ontario are essentially Case II waters.

The supporting hypothesis for this study is that in complex Case II Great Lakes waters (near shore, Bays and most of Lakes Erie and Ontario) a full spectrum, multiple CPA component retrieval approach provides more accurate chl concentration estimates than traditional chl specific oceanic band ratio techniques. To successfully estimate chl, doc, and sm concentrations in Case II water, detailed knowledge of the inherent optical properties (IOPs) for these three CPAs is required (Bukata et al., 1995). The specific objectives of this study included: 1) generation, evaluation, and documentation of individual HO models, and their differences, for each Great Lake; 2) comparison of the performance of each individual lake HO based retrieval with an average HO model used on all five lakes; 3) comparison of the results with the band ratio OC3 algorithm that assumes the Great Lakes color is dominated by phytoplankton; and 4) assess several atmospheric correction procedures using in situ observations to optimize CPA-A concentration retrievals. This paper presents the CPA algorithm that can use MODIS, SeaWiFS, MERIS, and VIIRS satellite data to estimate concentrations of chl, doc, and sm for the Great Lakes. The algorithm is based on new individual lake specific hydro-optical models and uses the Levenberg–Marquardt (L–M) procedure described in detail by Korosov et al. (2009). The individual lake HO coefficients used by the CPA-A are described and compared. Algorithm retrieval values for each lake are presented along with comparisons to in situ chl concentrations provided by EPA field campaigns. Additionally, the chl retrievals for the lakes are compared to the band ratio OC3 chl estimates. The paper also discusses the procedure used to process the data from the NASA archives to generate the retrievals from the MODIS data including a suggested operational atmospheric correction for the Great Lakes.

### Hydro-optical model generation and algorithm description

The overall algorithm and initial evaluation are described by Pozdnyakov et al. (2005), Shuchman et al. (2006), and Korosov et al. (2009) and will not be repeated here. In summary, the model assumes that the remote sensing reflectance ( $R_{rs}$ ) can be calculated from the specific (chl, doc, sm) absorption and backscattering coefficients (Jerome et al., 1996), along with concentrations of each CPA:

$$\begin{aligned} R_{rs,i} &= -0.00036 + 0.110(b_i/a_i) - 0.0447(b_i/a_i)^2 \\ a_i &= a_{H2O,i} + C_{chl}a_{chl,i} + C_{doc,i}a_{doc,i} + C_{sm}a_{sm,i} \\ b_i &= b_{H2O,i} + C_{chl}b_{chl,i} + C_{sm}b_{sm,i} \end{aligned}$$

where,

$C$	Vector representing concentrations of each CPA
$a_i$	Bulk absorption coefficient for each CPA at band i
$b_i$	Bulk backscattering coefficient for each CPA at band i
$a_{ij}$	Specific absorption coefficient for each CPA j at band i
$b_{ij}$	Specific backscattering coefficient for each CPA j at band i.

As the above equations indicate, specific absorption and backscattering coefficients for each CPA are needed for each satellite spectral band used in the algorithm. The table of specific backscattering and absorption coefficients is referred to as the HO model. The original algorithm used for the SeaWiFS seven year time series analysis of Lake Michigan (Shuchman et al., 2006) utilized a HO model developed in the 1990s by Bukata et al. (1995) for Lakes Ontario and Ladoga. This HO model when used to analyze the data of Lake Michigan correctly predicted the relative seasonal and annual changes in chl but under predicted by a large amount of the measured concentration. The algorithm also was able to capture important episodic events and temporal-spatial phenomena that scheduled field sampling cannot capture, such as the spring time sediment re-suspension event in Lake Michigan. The doc and sm

concentration estimates for Lake Michigan compared quite favorably with the field data (Shuchman et al., 2006).

The optical data used to generate and validate the absorption and backscattering coefficients were obtained using the NOAA–GLERL Satlantic Profiling multi-channel Radiometer (SPMR) and the Multi-channel Surface Reference (SMSR) instrument package (see [www.Satlantic.com](http://www.Satlantic.com)). The SPMR is equipped with 2 OCP-1000 optical sensors, an external pressure sensor, two internal optical sensors and a sensor to measure tilt. The SMSR contains 2 OCP-1000 optical sensors, 2 axis tilt sensors, and 2 internal optical sensors. Light is recorded in micro watts per cm squared per nanometer, with a spectral location accuracy of approximately plus or minus 0.2 nm. Channels used for all light data collected were from SeaWiFS and MODIS color bands which include: 411.3, 443.1, 470.4, 490.5, 510.7, 532.1, 554.3, 665.6, and 683.5 nm. During deployment the vertical rate of descent of the profiler was kept between 0.7 m/s to 1 m/s while the surface reference is deployed concurrently on the water surface to measure total incident downwelling irradiance ( $E_s$ ). Deployment of the instruments occurred from the GLERL R/V Shenehon, EPA R/V Lake Guardian, and other research vessels of opportunity on the Great Lakes in collaboration with the Upstate Freshwater Institute (UFI). The Satlantic Profiler measures  $E_d$  (downwelling irradiance) and  $L_u$  (upwelling radiance). The Satlantic Surface Reference measures  $E_s$  (total incident downwelling irradiance) and  $L_u$  (upwelling radiance). Derived from these basic measurements are higher level measures including Remote Sensing Reflectance, Diffuse Attenuation Coefficients, Photosynthetically Available Radiation (PAR), and Chlorophyll-a ([www.satlantic.com](http://www.satlantic.com)). These optical measurements are used to validate the HO parameters through the inverse radiative transfer function with the absence of atmospheric signal contribution. They can also be inverted into absorption and backscatter components to potentially be used in the HO models as well if sufficient measurements exist for robust optimization of these parameters.

In addition to the above described Satlantic measurements, a Satlantic with all visible bands in the 400 to 700 nm range, a BB-9 to measure backscatter, and AC-S for absorption characterization were deployed by the Upstate Freshwater Institute (UFI) during a series of EPA and NOAA GLERL cruises. The in situ measurements of chl, cdom, sm absorption and backscatter obtained by the AC-S and BB-9 instruments were particularly useful in generating the new HO models. Coincident with each optical set of measurements was a series of water collections which included measurements of total suspended matter and inorganic suspended matter, chlorophyll, and dissolved organic carbon (doc/tog). Total suspended matter (tsm) was measured by filtering lake water through combusted, rinsed, dried, and weighted 47 mm GF/F glass fiber filters. The same water sample was also used to determine the contribution of inorganic material by reweighting the final sample after high temperature combustion. Volumes of water filtered varied between 200 and 2000 ml depending on the particle load and water was filtered until the filter became visually clogged. To obtain the required in situ chlorophyll measurement a standard procedure was used, where triplicate samples of 100 ml of water were filtered through a Whatman, 47 mm, GF/F filter. After filtering, the filter was immediately placed into a 14 ml polypropylene Falcon tube, where it was capped and frozen in a dark environment until analysis. Chlorophyll was analyzed using the Speziale et al. (1984) Dimethylformamide (DMF) method. Water for the doc measurement was processed by filtering lakewater through a 25 mm precombusted (400 °C for 4 h) GF/F filter and poured in triplicate glass tubes for analysis. The dissolved organic carbon was analyzed via the high temperature combustion method #5310 B from the Standard Methods for the Examination of Water and Wastewater 20th Edition (1998). The doc was also measured using the Shimadzu TOC5000 ([www.ssi.shimadzu.com/products/products.cfm?subcatlink=tocanalyzers](http://www.ssi.shimadzu.com/products/products.cfm?subcatlink=tocanalyzers)) which defines total carbon as “non-purgeable organic carbon” (npoc).

The in situ optical and laboratory data was then used to generate absorption coefficients for chl, doc, and sm for all five lakes. Presently, the

original [Bukata et al. \(1995\)](#) backscatter coefficients for chl and sm are being used in the new set of algorithms. The backscatter values for sm in the open part of the Great Lakes should not have changed significantly since the 1990s while this may not be true for chl. There is the potential for significantly different sm backscatter coefficients between varying sediment particle sizes (e.g. river discharge clay particles or re-suspended quartz sand sediment particles) which can dramatically influence retrieval concentrations particularly in the near shore. In the near future the UFI BB-9 will be used to update the chl backscatter coefficients for each of the five Great Lakes.

Specific CPA absorption coefficients were derived from in situ measurements of the absorption of chl, cdom, and sm at known concentration levels. In order to derive the specific cross sections used as the HO model coefficients, both bulk absorption ( $a$ ) and backscatter ( $b$ ) must be partitioned into individual components (i.e.  $a(\text{chl})$ ,  $a(\text{sm})$ ,  $a(\text{cdom})$ ,  $b(\text{chl})$ ,  $b(\text{sm})$ ). This partitioning was provided by the Upstate Freshwater Institute (UFI) in accordance to the methods described by [Effler et al. \(2010\)](#) and [Peng et al. \(2009, 2011\)](#). The individual partitioned absorption of chl, cdom, and sm for each spectral band is then divided by the corresponding concentrations of each CPA to derive the HO model absorption cross section coefficients. Absorption coefficients were calculated for every sample within a single lake and then averaged together to account for the slight IOP variations.

The CPA-retrieval generates concentration values for chl, doc and sm. As discussed previously, ocean color satellite sensor observations of water leaving radiance are influenced by the presence of cdom, the colored portion of the total dissolved organic carbon and the only part of doc that absorbs light. Presently cdom values in the Great Lakes are reported in units of absorption ( $\text{m}^{-1}$ ) and there is no robust generalized relationship between cdom and doc concentrations. In order to retrieve concentration estimates of doc, which is the desired water quality parameter, the specific HO doc absorption coefficient ( $a(\text{doc})^*$ ) parameter was defined as  $a(\text{cdom})$  divided by the doc concentration ([Binding et al., 2008; Bukata et al., 1983](#)). These individual coefficients which were obtained at various locations throughout each lake were then averaged to obtain a composite relationship between cdom and doc for a given Great Lake. This approach accounts for the variability in the cdom and doc relationship between each of the five Great Lakes as well as the variability ([Binding et al., 2008](#)) within a given lake. Further research is being conducted to better quantify cdom concentration from optical information, specifically using the absorption spectral slope.

The HO model chl, doc, and sm absorption coefficients generated from the in situ data for the individual lakes are compared with the original coefficients generated by [Bukata et al. \(1995\)](#) in Fig. 1. Examination of Fig. 1 demonstrates that different HO absorption coefficients are required for each lake or large water mass (i.e. different bodies of water

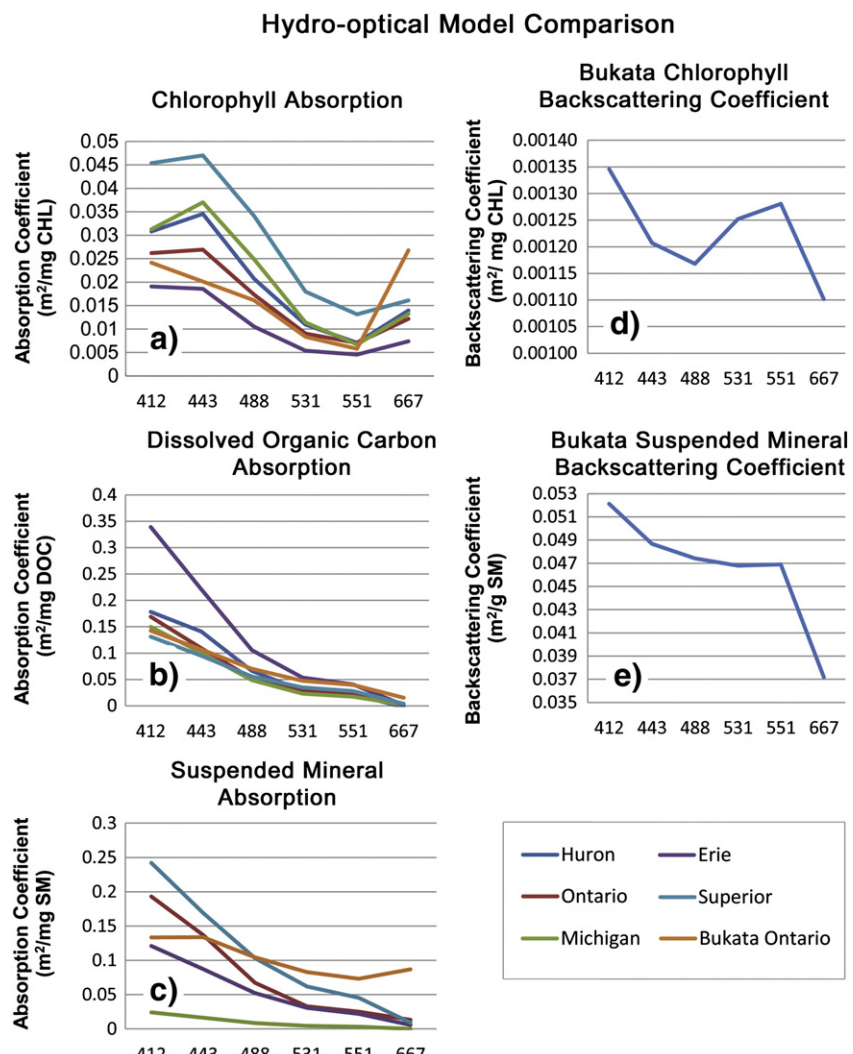


**Fig. 1.** New HO Absorption coefficients for all five of the Great Lakes as well as the scattering coefficients used. Panel a) chlorophyll absorption, b) doc absorption, c) sm absorption, d) chlorophyll backscatter, and e) sm backscatter (X axis in all panels is wavelengths ( $\lambda$ ) in nanometers). The original [Bukata et al. \(1995\)](#) absorption coefficients which are replaced in the new HO models are also included for comparison. The original backscatter coefficients for chl and sm generated by [Bukata et al. \(1995\)](#) are still used for all lakes in the new set of HO models.

have different IOPs). Similar types of water bodies such as Lakes Michigan and Huron exhibit similar but clearly discernible HO models. Clearly each HO model depends on what type of chlorophyll and accessory pigments, yellow substance, and inorganic sediment are in given water mass. The figure also demonstrates that there has been significant departure in the chl and the sm absorption coefficient values when compared to the 30 plus year old Bukata values. There are no sm absorption spectra for Lake Huron in Fig. 1 because of an insufficient number of in situ observations. Therefore, the Lake Michigan sm absorption was also used for Lake Huron in the CPA-A. These HO results are consistent with independent measurements of absorption and backscatter made by the Upstate Freshwater Institute (UFI) (O'Donnell et al., 2009).

The specific chlorophyll absorption coefficients (Fig. 1a) tend to decrease with change in trophic state (oligotrophic (Superior) to eutrophic (Erie)). This is likely due to the chlorophyll pigment and accessory pigment variability in the predominant phytoplankton species and size as reported in various studies (Lohrenz et al., 1999, 2004; Morel and Bricaud, 1986) that identified the change in absorption coefficients with algal species and cell composition. It is also expected that the specific chl coefficients will change throughout the vegetative season of a given year as the dominant chlorophyll containing species changes with average lake temperature. This has been observed in the case of cold water upwelling events in Lake Michigan that bring a different sized phytoplankton, then present in the upper water, thus changing the specific chl absorption coefficients for those areas. The departure in Lake Ontario chl absorption between the historical Bukata coefficient and the newly derived value in the 443 and 667 nm wavelengths is likely due to differing phytoplankton species and their resulting particle size either from a lake wide phytoplankton regime shift or simply from localized events that manifested in the field samples (Lampman and Makarewicz, 1999). Further investigation into this is warranted. It should be noted how close the Lake Michigan and Huron chl absorption coefficients are through all wavelengths indicating very similar phytoplankton species compositions. This indicates that the HO models for lakes Michigan and Huron could potentially use the same chl absorption coefficient in the mid to late summer time frame, and this will be further evaluated. The specific doc absorption coefficient (Fig. 1b) for each lake shows remarkable similarity, except for Erie in the blue wavelengths, potentially indicating that a composite doc absorption coefficient could potentially be utilized for all Great Lakes. These findings are somewhat surprising given the more varying results shown in Lakes Erie (Binding et al., 2008) and Superior (Effler et al., 2010). The similarities in doc absorption coefficients could be the result of seasonal timing (August) when the in situ measurements were collected. It is reasonable to assume that these coefficients could vary significantly in the spring and fall when more river runoff is experienced as this is the primary delivery system for doc into the lakes.

The significant differences in sm absorption spectra between lakes are primarily due to their underlying geology and riparian land use. This is particularly evident in Lake Erie where sm composition is directly related to varying river discharge (Maumee vs. Detroit) and sediment re-suspension due to significant storm events. The differences in sm absorption between lakes Michigan and Ontario are at first disconcerting as their underlying geologies are essentially the same (i.e. Limestone) and one would expect similar sediment particle size. However the widespread abundance of zebra and quagga mussels in Lake Michigan is postulated to have diminished the amount of precipitated calcium carbonate from the water, similar to the observations in Lake Ontario (Barbiero et al., 2006).

As technology allows for partitioning of the bulk backscatter in to specific CPA coefficients better HO parameters can be derived leading to more robust retrievals. These technologies have been shown to have promise (Peng and Effler, 2011; Peng et al., 2009).

To summarize, the HO-model is a set of parameters that describe the optical conditions of a body of water, and is essential for the proper

operation of the CPA-A. The HO model as mentioned previously consists of the specific absorption and backscattering coefficients associated with each CPA. The coefficients relate the concentrations of each CPA to the total amount that chl, cdom, and sm absorb and backscatter in specific portions of the visible electromagnetic spectrum observed by the ocean color satellites.

Given that an accurate HO model can be generated from a body of water, CPA-A concentration images can be produced from satellite reflectance images using a multivariate inverse procedure. As mentioned previously, the CPA-A approach uses the Levenberg–Marquardt procedure

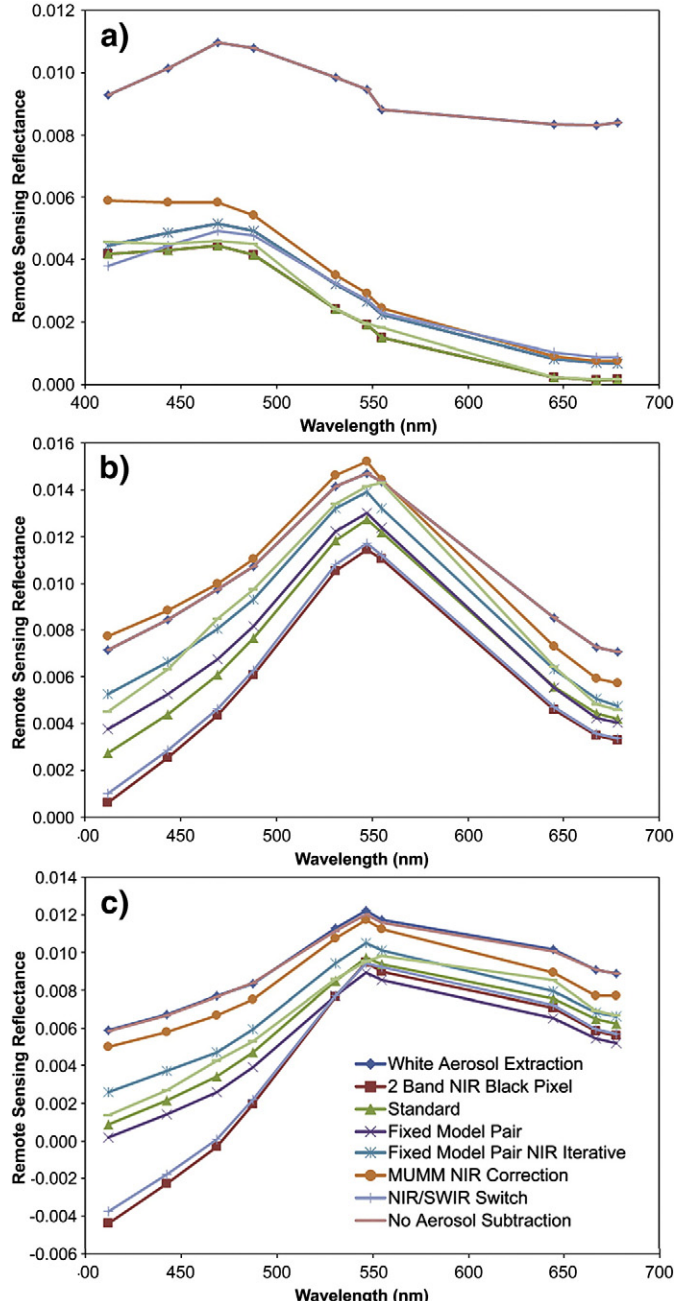


**Fig. 2.** Comparisons of MODIS reflectance values to near coincident (within 1 h) ship-based radiometer observations using the suite of atmospheric aerosol correction techniques for offshore Lake Huron water (a), a Lake Erie site with a high concentration of chlorophyll but not in a sediment plume (b), and a near shore site in Lake Erie located within a sediment plume (c). For all three cases the standard NASA correction performs well as does the 2 band NIR black pixel technique. Note the importance of correctly accounting for aerosols as well as observing the large differences in the reflectance in the blue portion of the spectrum as a function of the correction technique used. Correction techniques that produce negative or near zero reflectance values are unusable.

**Table 1**

Summary of the satellite image dates and EPA in situ measurements used in the evaluation. Note that all MODIS image dates are within 5 days of the corresponding EPA field campaign dates.

Lake	Year	MODIS	EPA
Michigan	2010	8/8	8/1–8/5
	2011	8/3	8/2–8/5
Huron	2010	8/12	8/6–8/8
	2011	8/11	8/6–8/8
Superior	2008	8/25	8/20–8/27
	2011	8/27	8/18–8/22
Erie	2009	8/14	8/17–8/20
	2010	8/7	8/9–8/11
Ontario	2008	8/6	8/11–8/13
	2011	8/8	8/12–8/14

for finding a solution to the inverse radiative transfer problem. In this procedure a CPA concentration vector is found which minimizes the error between the measured and calculated Rrs. After an initial educated estimate for the CPA concentrations, the L-M procedure converges on a minimum in the error function using:

$$\sum_{i=1}^{\text{Total Bands}} \left( \frac{S_i - Rrs_i}{S_i} \right)^2 = \text{Error}$$

where,

$S$  Measured remote sensing reflectance from satellite for band  $i$   
 $Rrs_i$  Calculated remote sensing reflectance from CPA concentrations, HO-model for band  $i$ .

### Atmospheric corrections

It is generally accepted that the atmosphere contributes more than 90% of the signal measured by ocean color satellite sensors (Siegel

et al., 2000) when the water is not extremely turbid or contains floating algal particles. Atmospheric signal is typically removed before bio-optical analysis is completed. Atmospheric correction for visible ocean or lake color satellite data includes corrections for sun glint, surface gravity waves (white caps), Rayleigh and aerosol scattering (Gordon and Wang, 1994). It is assumed that for relatively clear water NIR radiance is non-existent or below the noise threshold of the sensor and any NIR radiance detected must be from aerosol scattering effects. This is known as the Black Pixel Assumption (Gordon and Clark, 1981). Several aerosol models have been developed that relate NIR reflectance due to aerosols to radiances detected in the visible portions of the spectrum (Gordon and Wang, 1994). In some cases, atmospheric corrections produce negative radiances. These negative radiances can be a result of failure of the black pixel assumption, due to water constituents with significant NIR reflectance, or if absorbing aerosols are present. It is the failure to account correctly for absorbing aerosols that can affect the accuracy of the CPA-A retrievals.

Correctly accounting for the effect of the atmospheric path length is important in optimizing the CPA-A and OC3 chl retrievals. For the open portion of the lakes, one can assume that the aerosols are relatively constant throughout the path length of the lower troposphere and NIR reflectance due to water constituents is zero, hence the atmospheric correction is relatively straightforward and a number of algorithms work well (Gordon and Clark, 1981). To evaluate the importance of correcting for atmospheric effects, eight aerosol correction approaches including the recommended NIR/SWIR technique (Gordon and Wang, 1994; Ruddick et al., 2000; Siegel et al., 2000; Wang and Shi, 2007) for Case II waters was applied to three MODIS scenes that had near coincident (within 1 h) ship based radiometer measurements. For this atmospheric correction analysis MODIS images were processed from Level 1A to Level 2 with different aerosol correction methods using SeaDAS version 6.3. The three scenes included a Lake Huron open water image, a Lake Erie near shore chlorophyll dominated image and a Lake Erie sediment dominated image. These three selected datasets (low and high reflectivity) are representative of the types of water typically encountered in the Great Lakes and thus provide useful insight into an

**Table 2**

HO model coefficients generated from optical measurements for each individual lake. Also included for comparison are the original Bukata coefficients as well as coefficients averaged using the five individual lakes. Standard deviations (in parentheses), both between lakes and within lakes are also presented in the table.

	412 nm	443 nm	488 nm	531 nm	547 nm	667 nm
Chl absorption						
Huron	0.0308 (0.0096)	0.0346 (0.0105)	0.0206 (0.0077)	0.0109 (0.0027)	0.007 (0.0015)	0.0139 (0.0031)
Ontario	0.0261 (0.0173)	0.0269 (0.0199)	0.0173 (0.0124)	0.0090 (0.0061)	0.0070 (0.0061)	0.0121 (0.0056)
Michigan	0.0312 (0.0083)	0.0370 (0.0113)	0.0248 (0.0078)	0.0114 (0.0041)	0.0066 (0.0019)	0.0132 (0.0035)
Erie	0.0190 (0.0025)	0.0185 (0.0009)	0.0104 (0.0018)	0.0053 (0.0011)	0.0045 (0.0009)	0.0073 (0.0010)
Superior	0.0453 (0.0278)	0.0470 (0.0257)	0.0340 (0.0183)	0.0179 (0.0109)	0.0131 (0.0093)	0.0161 (0.0084)
Bukata Ontario	0.0241 (NA)	0.0201 (NA)	0.0161 (NA)	0.0083 (NA)	0.0058 (NA)	0.0268 (NA)
All lake average	0.0292 (0.0089)	0.0299 (0.0109)	0.0205 (0.0081)	0.0104 (0.0042)	0.0074 (0.0029)	0.0151 (0.0065)
Sm absorption						
Huron	0.0239 (0.0108)	0.0162 (0.0073)	0.0084 (0.0039)	0.0042 (0.0020)	0.0033 (0.0015)	.0001 (0.000)
Ontario	0.1931 (0.2066)	0.1368 (0.1477)	0.0672 (0.0764)	0.0327 (0.0409)	0.0249 (0.0305)	0.0132 (0.0136)
Michigan	0.0239 (0.0108)	0.0162 (0.0073)	0.0084 (0.0039)	0.0042 (0.0020)	0.0033 (0.0015)	.0001 (0.000)
Erie	0.1209 (0.0739)	0.0870 (0.0597)	0.0521 (0.0406)	0.0307 (0.0260)	0.0220 (0.0197)	0.0056 (0.0042)
Superior	0.2419 (0.3234)	0.1688 (0.2328)	0.1029 (0.1442)	0.0617 (0.0873)	0.0452 (0.0661)	0.0090 (0.0148)
Bukata Ontario	0.1332 (NA)	0.1335 (NA)	0.1042 (NA)	0.0829 (NA)	0.0731 (NA)	0.0867 (NA)
All lake average	0.1228 (0.0881)	0.0931 (0.0650)	0.0572 (0.0428)	0.0361 (0.0313)	0.0286 (0.0268)	0.0191 (0.0335)
Doc absorption						
Huron	0.1782 (0.0863)	0.1408 (0.0599)	0.0662 (0.0345)	0.0285 (0.0211)	0.0214 (0.0158)	0.0019 (0.0026)
Ontario	0.1687 (0.0484)	0.1089 (0.0321)	0.0513 (0.0166)	0.0278 (0.0095)	0.0232 (0.0074)	0.0041 (0.0014)
Michigan	0.1496 (0.0690)	0.1004 (0.0379)	0.0485 (0.0199)	0.0228 (0.0117)	0.0173 (0.0086)	0.0017 (0.0014)
Erie	0.3392 (0.1323)	0.2210 (0.0848)	0.1057 (0.0416)	0.0537 (0.0219)	0.0404 (0.0171)	0.0014 (0.0046)
Superior	0.1312 (0.0539)	0.0951 (0.0397)	0.0554 (0.0258)	0.0349 (0.0175)	0.0281 (0.0139)	0.0040 (0.0018)
Bukata Ontario	0.1425 (NA)	0.1069 (NA)	0.0701 (NA)	0.0475 (NA)	0.0396 (NA)	0.0153 (NA)
All lake average	0.1849 (0.0775)	0.1289 (0.0478)	0.0662 (0.0210)	0.0359 (0.0121)	0.0283 (0.0096)	0.0048 (0.0053)
Pure water absorption	0.0161	0.0143	0.0182	0.0416	0.0548	0.4211
Pure water backscatter	0.0025	0.0019	0.0012	0.0008	0.0007	0.0003
Bukata Chl backscatter	0.0013	0.0012	0.0012	0.0013	0.0013	0.0011
Bukata Sm backscatter	0.0521	0.0487	0.0474	0.0468	0.0469	0.0372

**Table 3**

$r^2$  and RMSE values that summarize the accuracy of the CPA-A and OC3 chl concentration retrievals for each individual lake, using individual lake HO models, as compared to EPA in situ observations. Both techniques produced acceptable retrievals with the exception of the OC3 in Lake Erie. Also presented are the in situ chlorophyll mean and standard deviation for each lake as well as the CPA-A and OC3 modeled mean and standard deviation. The CPA-A and OC3 line of best fit model equation with respect to the in situ data is also provided.

Lake	# sites	CPA-A $r^2$	CPA-A RMSE	OC3 $r^2$	OC3 RMSE	EPA CHL mean	EPA CHL st. dev.	CPA-A CHL mean	CPA-A CHL st. dev.	OC3 CHL mean	OC3 CHL st. dev.	CPA-A model Equation	OC3 model Equation
Superior	34	0.49	0.15	0.45	0.36	0.85	0.22	0.83	0.22	0.90	0.49	0.71x + 0.23	1.53x–0.39
Michigan	19	0.78	0.27	0.74	0.48	0.78	0.41	0.79	0.58	0.74	0.96	1.24x–0.17	1.99x–0.81
Huron	25	0.69	0.13	0.71	0.19	0.52	0.21	0.53	0.24	0.45	0.36	0.96x + 0.03	1.48x–0.32
Erie	39	0.55	2.18	0.20	9.11	5.24	3.81	4.96	3.29	9.64	10.29	0.64x + 1.61	1.19x + 3.39
Ontario	15	0.08	0.82	0.04	0.83	2.54	0.64	2.87	0.88	2.27	0.88	–0.40x + 3.87	0.28x + 1.57

operational atmospheric correction procedure for Great Lakes retrievals. Fig. 2 shows plots of MODIS and the ship based reflectance versus wavelength for the three different water types.

The Lake Huron MODIS radiance data corrected and converted to remote sensing reflectance using the eight primary aerosol correction approaches (available to SeaDAS users) for water remote sensing applications are shown in Fig. 2a along with the Satlantic reflectance values collected in situ within 1 h of the satellite overpass. For each of the eight MODIS aerosol correction methods an average reflectance value at the research vessel's location was generated. The average reflectance represented a 3-by-3 km area centered on the ship location. The averaging was done to account for temporal offsets, ship drift, and to improve the signal to noise ratio. The data from Lake Huron the assumption that for open water lake areas where reflectance values are expected to be relatively low (i.e. minimal NIR signal) the standard iterative NIR atmospheric correction can be used. The two band NIR black pixel technique also does an excellent correction, again due to minimal NIR signal, while the fixed model pair NIR iterative and NIR/SWIR switch corrections provide acceptable results. Not correcting for aerosols produces unrealistically high reflectance values (Fig. 2). For this open Lake Huron case the standard correction works well for all wavelengths, which in turn will generate acceptable CPA-A and OC3 retrievals.

A Western Lake Erie (extreme Case II water) MODIS data set was also evaluated using the eight aerosol correction approaches. Two sites with different dominant water constituents (chl vs. sm) were analyzed to determine the effects that atmospheric corrections have on different water colors. Fig. 2b is a plot that summarizes the satellite and ship based reflectance spectra in this low sediment but high-chlorophyll concentration water. The Fixed Model Pair NIR Iterative aerosol correction method best matches the radiance profile from the in situ radiometer. The NASA standard aerosol model also closely follows the in situ measurements as well, indicating that several correction methods will provide reasonable chlorophyll estimates in this type of water. The smaller difference between no aerosol correction and the standard corrected reflectance is contrary to the relationship shown in the Lake Huron example (Fig. 2a). In this case the two band NIR black pixel and NIR/SWIR switch produced near negative reflectance in the blue wavelengths, thus rendering those bands not useful in any retrieval algorithm. This Lake Erie example demonstrated the large variability in the reflectance in the blue portion of the spectra that can result as a function of the correction technique used.

The second example from western Lake Erie (Fig. 2c) compares satellite observed and in situ reflectance values in sediment laden water approximately 4 km from shore. The NASA standard and Fixed Model Pair aerosol models compare best with the in situ field reflectance measurements, with the fixed model pair NIR iterative also providing a reasonable correction. Negative radiance values resulted for the MODIS blue channels when using the NIR/SWIR and NIR Black Pixel aerosol models. Negative radiance values will significantly reduce the ability to retrieve accurate chlorophyll, sm, and doc concentrations in sediment laden waters.

In summary, the atmospheric correction analysis strongly suggests that the NASA standard aerosol model will provide accurate reflectance that can then be used to retrieve reliable chlorophyll concentrations. It

should be noted that only three cases were evaluated and additional sites in close proximity (1–2 km) of the shore need to be evaluated. Negative radiance values in the blue bands have resulted, in close proximity to the shoreline, using the standard aerosol correction, hence the need for additional evaluations. Additionally floating algal mats as commonly observed in the Western basin of Lake Erie also adversely affect the corrected radiance values due to significant NIR return. An interesting result of the atmospheric correction reveals that the use of NIR/SWIR switch and two band NIR black pixel methods are not particularly useful in correcting the two Lake Erie examples. This observation is contrary to the assumption that this correction algorithm is preferred in very turbid, Case II water. Since MERIS does not have a SWIR band, it is useful that this analysis does not support a NIR/SWIR approach. The large disagreement of corrected reflectance values as a result of the different algorithms in the blue region of the spectrum is also worthy of note. In turbid waters, we typically do not use the blue bands in the CPA-A retrieval, partially due to the poor performance of the atmospheric correction in the blue wavelengths.

### Image acquisition and processing

The findings from the atmospheric correction analysis presented previously confirmed the appropriateness of utilizing the standard aerosol correction for ocean color remote sensing in the Great Lakes. Because no alternative atmospheric correction procedures or alteration of the downstream product models were necessary, it was concluded that using the standard NASA level 2 (L2) data downloaded directly from the OceanColor WEB portal (<http://oceancolor.gsfc.nasa.gov/>) was indeed appropriate and relevant to the greater user community. This approach is advantageous as the standard L2 data is easy to obtain and use without many preprocessing steps which require detailed knowledge of processing software (SeaDAS) as well as the underlying optical properties of the data.

Thus data was acquired from the NASA OceanColor WEB Portal using the Level 1 and Level 2 browser. Cloud free imagery for each lake that was closest to the coincident EPA sampling data was identified and obtained. The definition of a cloud free image for this study is approximately 75% of pixels free of cloud contamination over the water. The

**Table 4**

$r^2$  and RMSE values that summarize the accuracy of the CPA-A chl concentration retrievals using an average all lake HO model for each individual lake as compared to EPA in situ observations. Examination of the  $r^2$  and RMSE values indicates an all lake HO model produces less accurate chl estimates than a lake specific HO model (Table 3). Also presented are the CPA-A modeled mean and standard deviation for each lake as well as the line of best fit model equation with respect to the in situ data.

Lake	# sites	CPA $r^2$	CPA RMSE	CPA-A CHL mean	CPA-A CHL st. dev.	CPA-A model equation
Superior	34	0.05	0.32	0.46	0.33	0.35x + 0.17
Michigan	19	0.43	0.49	0.54	0.67	0.97x–0.26
Huron	11	0.06	0.04	0.15	0.05	–0.10x + 0.19
Erie	18	0.11	0.94	0.89	1.03	0.04x + 0.56
Ontario	15	0.03	0.74	1.75	0.78	0.23x + 1.18

selected imagery was then processed through the CPA-A to derive chl, sm, and doc concentrations. While running the CPA-A on a single pixel, or single spectral profile is not computationally intensive, running the algorithm on a large number of spectral signatures (e.g. a whole lake image) requires large quantities of allocated memory and processor computations. Therefore, the CPA-A is implemented using C++ and is run on a 128 core cluster supercomputer to optimize run times on large images. This facilitates the rapid processing of particular images during algorithm tuning and modification to quickly understand the effects of varying parameters on retrieved concentrations. It is possible to implement the CPA-A on stand-alone desktop systems with standard operating systems (e.g. Windows, Linux) with longer runtimes. The algorithm warps the image geospatially to a user defined coordinate system using the Geospatial Data Abstraction Library (GDAL) (<http://www.gdal.org/>) to ensure high spatial location accuracy for point comparisons. The OC3 chlorophyll product was extracted from the identical L2 data the CPA-A was applied to, and projected using GDAL.

The CPA-A retrieval uses the six visible ocean color sensing bands of MODIS (bands 8–13) to generate concentrations. In most cases, typically in the open, offshore, portions of the lakes all six bands are used to resolve the minimum error between measured and modeled reflectance. In some cases when the target (i.e. lake) is on the very East or West edge of the MODIS swath, significant striping manifests in the image retrievals. This is attributed to the known mirror-side banding and detector-to-detector striping issues associated with the MODIS sensor characterization and calibration. The banding is predominantly in the shorter (412 nm, 440 nm) blue wavelengths and as mentioned

previously, typically is more noticeable when the target is on the image edge. The banding is less noticeable in Lake Erie where the water reflectance values are greater than the other lakes and not as adversely affected by the multipath loss at the image edges. For this reason, images are typically selected for processing when the target is located near the middle of the swath. If an image must be processed that is near the swath edge, the shortest blue band (412 nm) is not used in the retrieval. Efforts are ongoing to quantify how retrieval accuracies vary when different band combinations are used input into the algorithm.

Point comparisons between CPA-A chlorophyll and OC3 chlorophyll retrievals were accomplished using ArcGIS spatial analysis tools. The EPA chlorophyll concentrations used in the validation were obtained from the Great Lakes Environmental Database (GLEND) and processed to represent the near surface concentrations that are comparable to the satellite water color retrievals. In this case EPA chlorophyll observations were averaged within the top 3 m of the water column which corresponds to the attenuation length of Lake Michigan water and therefore detectable by satellite sensors (Bukata et al., 1995). Once these values were determined they were converted to points based on their recorded latitude and longitude coordinates. The chl values used in the algorithm validation are therefore distinctly different than the values used to create the HO models. In order to overcome the mixed pixel problem as well as the temporal offset between sampling data and satellite retrieval, a 3-by-3 kilometer buffer was applied to each sampling point. These buffers were then used to extract pixel values from the retrieval images which were then averaged to produce a comparable chl retrieval estimate for both CPA-A and OC3.

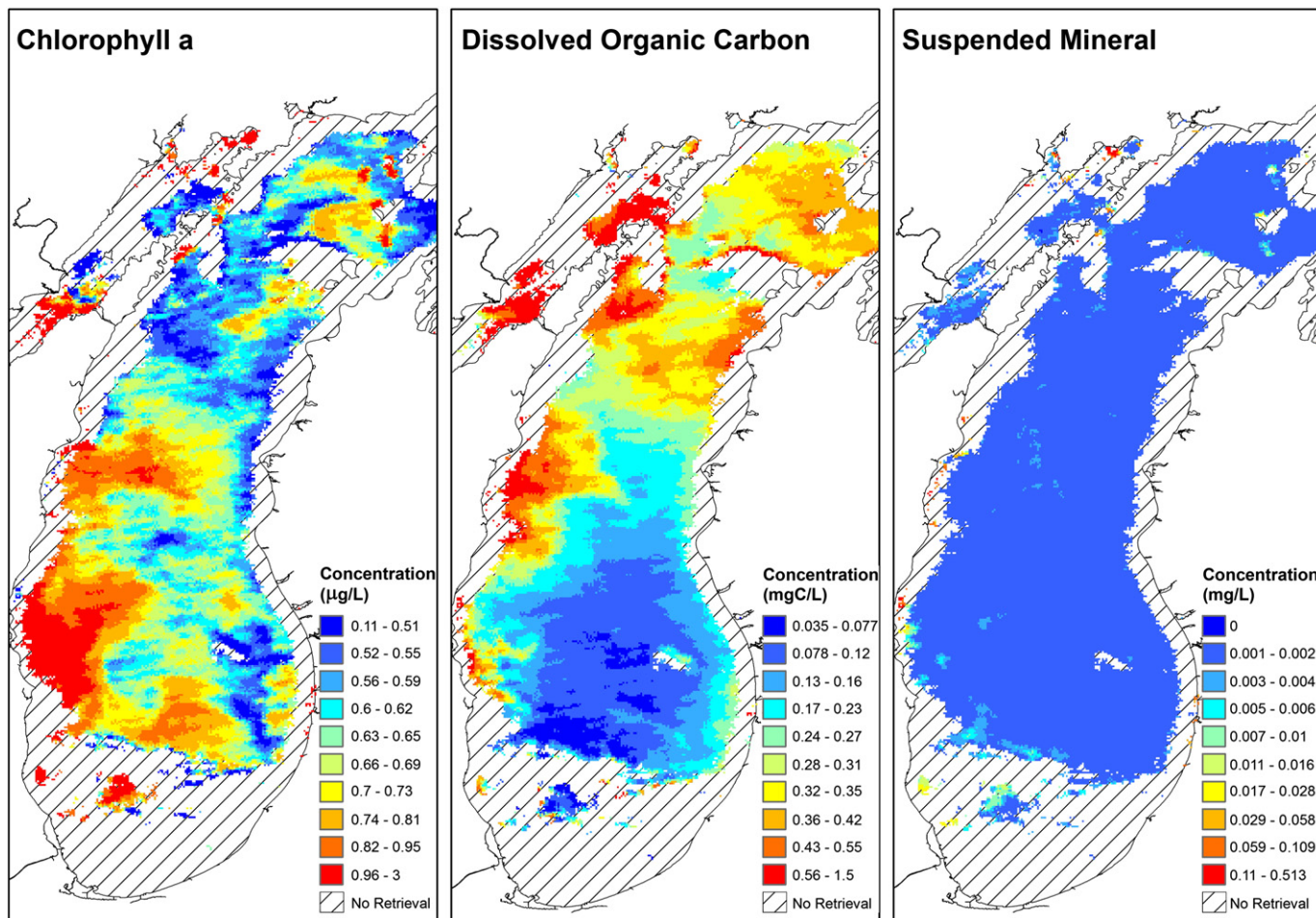


**Fig. 3.** August 8, 2010 Lake Michigan CPA-A Retrievals showing higher concentrations of chl and doc on the western side of the lake. The sm map shows low concentration of inorganic matter (sm) throughout the lake. A legend indicating the concentration of each CPA appears to the right of each map. The hatched areas indicate no CPA-A retrieval either due to cloud cover or optically shallow water.

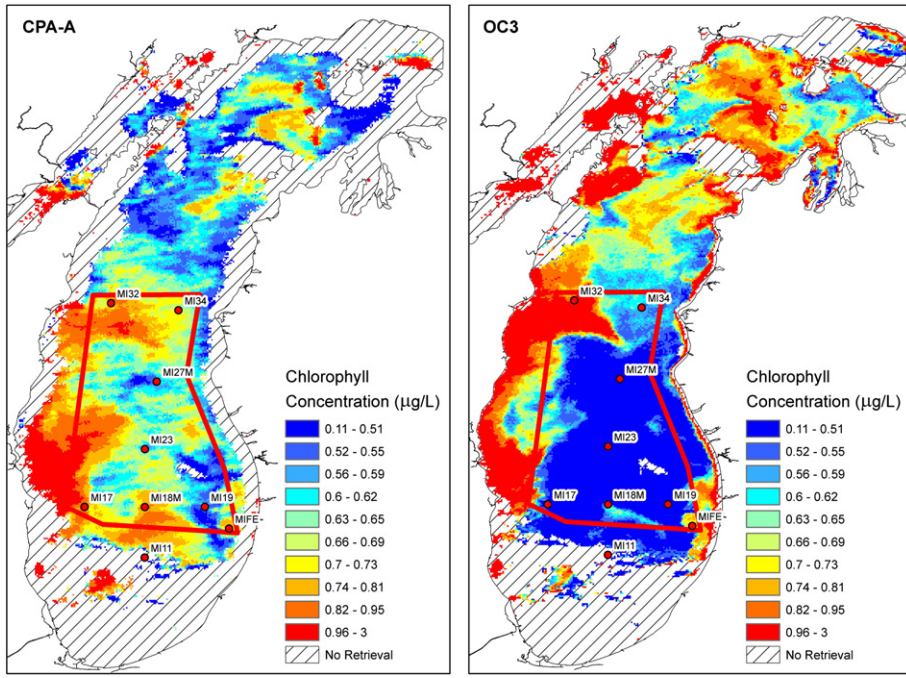


**Fig. 4.** Comparison between August 8, 2010 CPA-A and NASA standard OC3 chlorophyll concentration retrievals for Lake Michigan. A legend for the concentration values which are not on the same color scale for each retrieval appears to the right of each map. The red dots represent the locations of the EPA stations while the red box is the area used to compare the average chl value from the two techniques (EPA 8 stations 0.66 µg/L; CPA-A area average 0.69 µg/L; OC3 area average 0.42 µg/L).

Water quality measurements reported to the Great Lakes Environmental Database (GLEND) and used as validation in evaluation of the new algorithms are collected following the Great Lakes National Program

Office's (GLNPO) Water Quality Survey (WQS) Quality Assurance Project Plan (QAPP) submitted to the EPA. The measurements taken through the WQS are obtained through multiple devices. Physical and chemical sam-

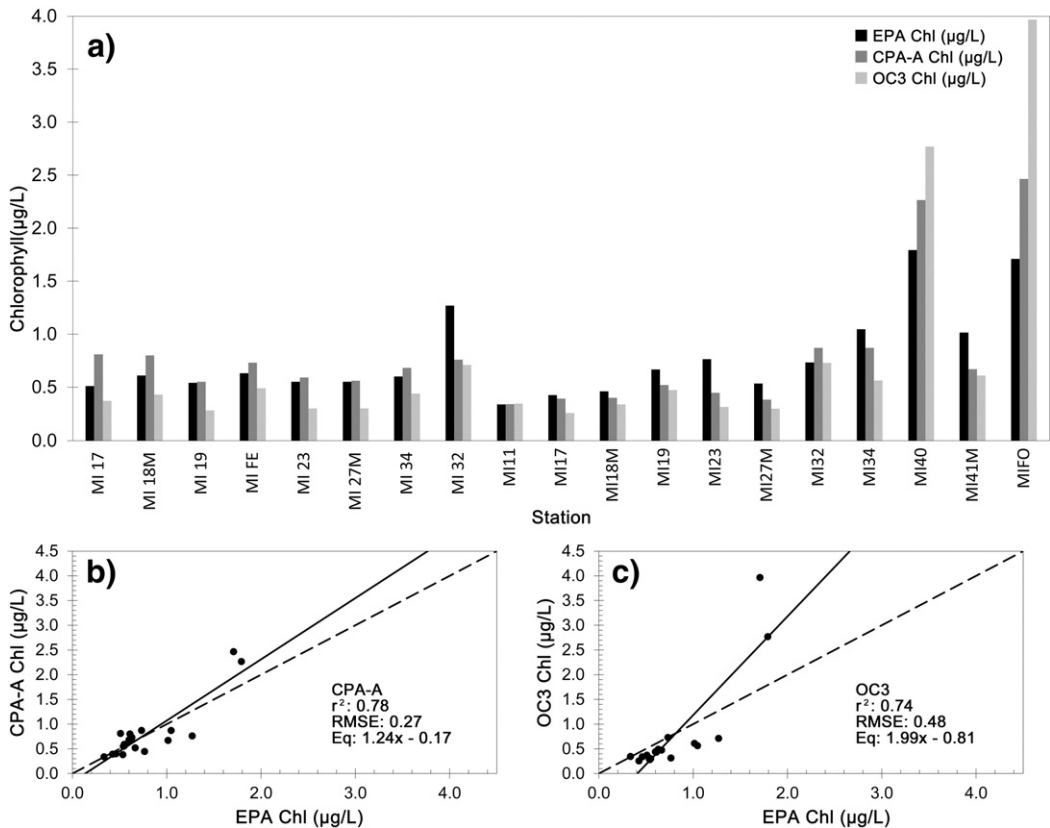


**Fig. 5.** Comparison of the Lake Michigan EPA in situ chl values (red dots in Fig. 4) to the CPA-A and OC3 derived estimates for the standard field campaign years 2010 and 2011. Shown in the figure are a) bar chart of CPA-A, OC3, and EPA chl concentrations at each station; b) scatterplot of CPA-A versus EPA chl values; and c) a scatterplot of OC3 versus EPA chl values. For each scatterplot  $r^2$  and RMSE values, as well as the line of best fit model equation are given. The line of best fit (solid line) and one-to-one line (dashed line) are shown on the scatterplots. Note that the vertical scales on the scatterplots are not all the same.

ples are obtained with a 12-bottle Rosette sampler system (SeaBird Electronics Carousel Water Sampler) that is used to measure the following water quality parameters: all nutrients, chlorophyll, dissolved oxygen, temperature, turbidity, specific conductance, pH, cations (calcium, magnesium, sodium), and total suspended solids. In addition to the parameters collected with the 12-bottle Rosette sampler, secchi disk readings are also recorded. All water quality measurements listed in the GLNPO WQS QAPP follow the Sampling and Analytical Procedures for GLNPO's Open Lake Water Quality Survey of the Great Lakes (<http://www.epa.gov/glnpo/monitoring/sop/index.html>) manual.

#### Algorithm results – comparisons to in situ measurements and the standard NASA OC3 retrieval

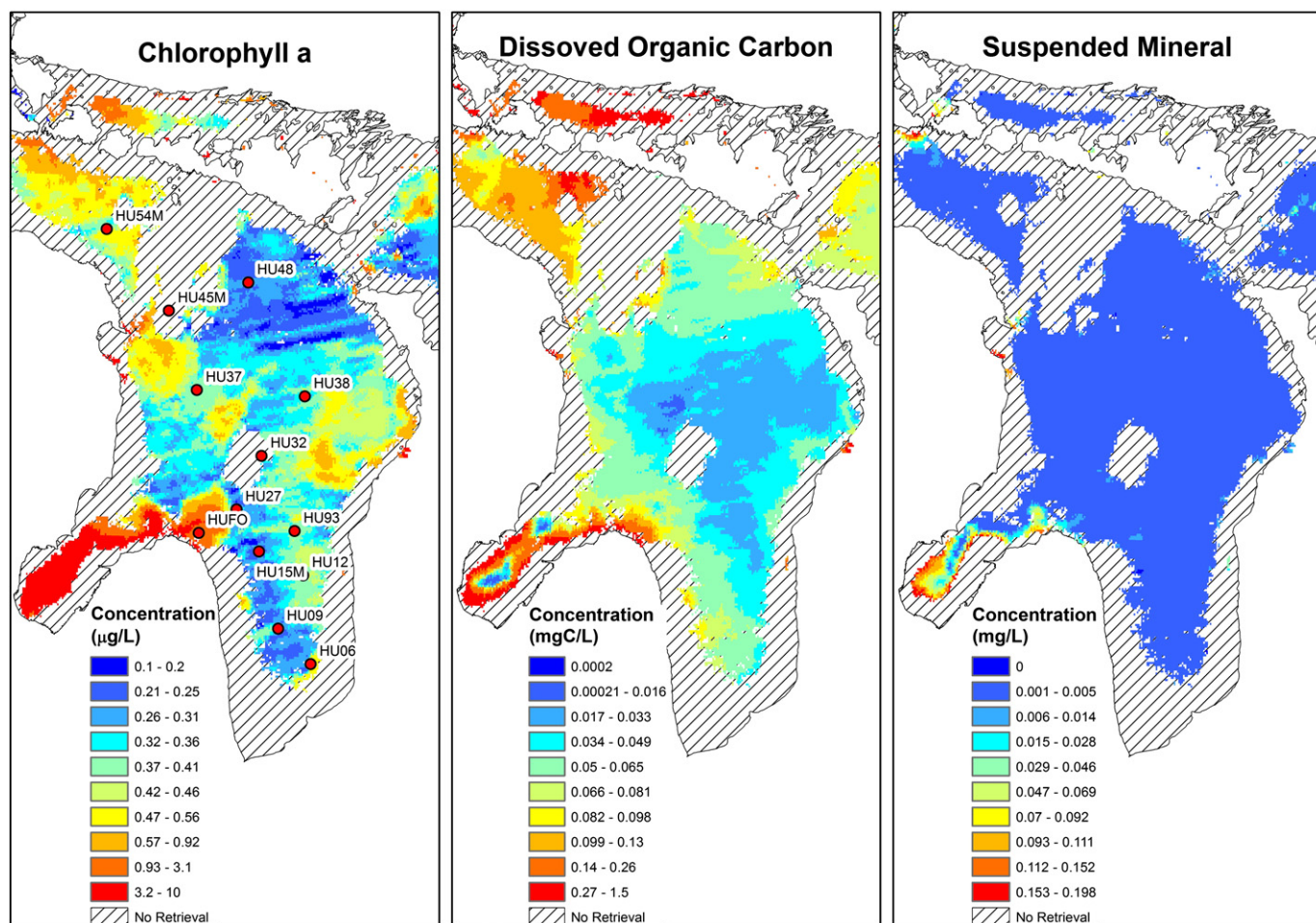
This section of the paper presents the retrieval results of the new CPA-A. The CPA-A chl values are compared to the near coincident EPA field campaign observations. The EPA does not routinely measure doc or sm. In the case of doc the UFI measurements not used in the HO model development were used to show that the CPA-A produces reasonable values. Additionally the CPA-A chl estimates are also evaluated in respect to chl concentration provided by the OC3 algorithm.

The dates of the satellite images selected for CPA-A and OC3 chl retrieval comparisons were based on near cloud free data acquisitions that occurred during or within a few days (0–5) of the standard Great Lakes EPA field campaigns of the R/V Lake Guardian. Table 1 summarizes the dates of the satellite images and EPA field campaign in situ

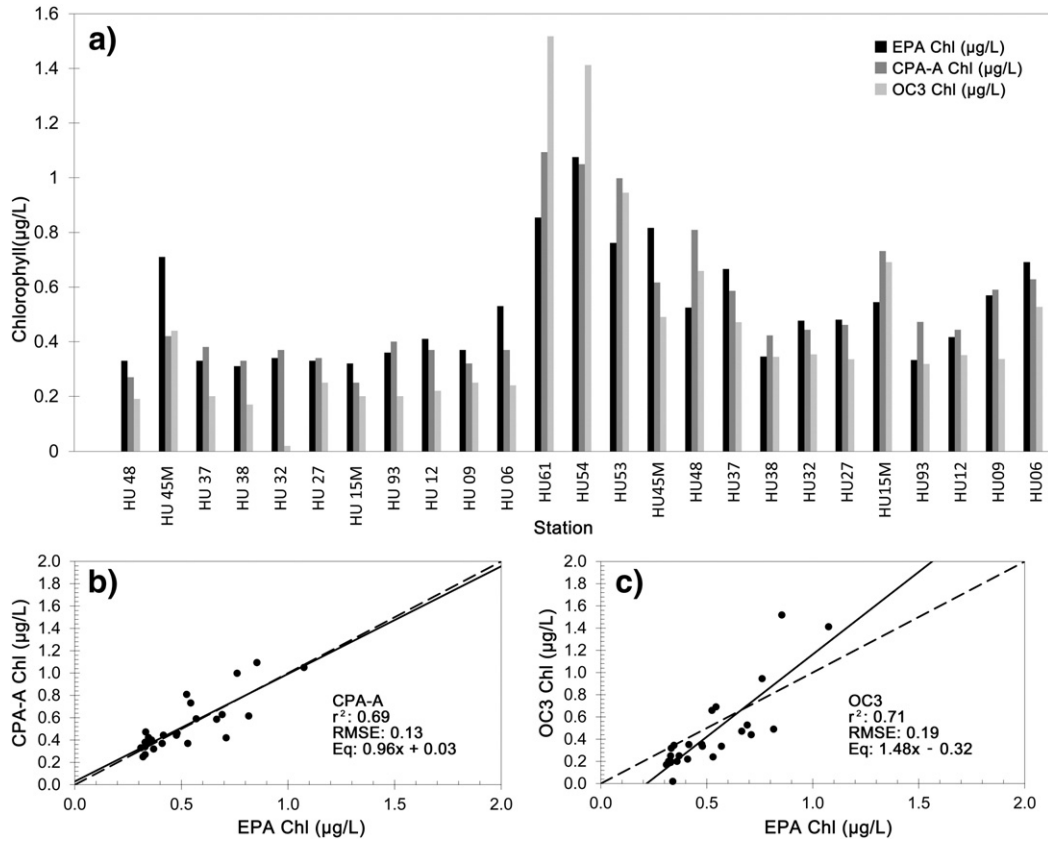
observations used in this study. The number of comparisons between the CPA-A and OC3 derived chl concentrations with EPA in situ data is limited in part due to lack of quality coincident cloud free imagery; however, for each lake, two years and two satellite image dates are compared.

Table 2 presents the HO coefficients generated from optical measurements for each individual lake. These values were extracted from Fig. 1 with the values for pure water also given. The historical Bukata coefficients are also presented to note the differences in these values over a 30 plus year period. Composite coefficients representing all lakes were also generated by averaging the five lake individual set of values and are included in the table. The standard deviation, per wavelength, between each lake HO parameter is also shown in the table. The standard deviations were derived from the average HO coefficients for each lake, including the historical Bukata Ontario values and indicate the variability of a given HO parameter between each lake. The largest standard deviations occur in the two shortest blue wavelengths (412 and 443 nm) due primarily to the drastic differences in CPA assemblages between lakes. Overall, there are similarities between the five-lake average coefficients and the individual Lake Ontario values. Also shown in the table, in parentheses, are the within lake standard deviations for each HO parameter, per wavelength and show small deviations per lake supporting the supposition that individual lake HO models are necessary to minimize retrieval errors.

Table 3 presents the lake, the number of sites used in the comparison, the  $r^2$  generated using the CPA-A when compared to the EPA in



**Fig. 6.** Lake Huron CPA-A Retrievals for an August 12, 2010 MODIS image. The hatched areas indicate areas of no CPA-A retrieval due to cloud cover or return from the lake bottom. Legends for the concentration values appear next to each map. The EPA sampling locations are shown as red dots in the figure.



**Fig. 7.** Comparison of the Lake Huron EPA in situ chl values to the CPA-A and OC3 derived estimates for the standard field campaign years 2010 and 2011. Shown in the figure is a) a bar chart of CPA-A, OC3, and EPA chl concentrations at each station; b) a scatterplot of CPA-A versus EPA chl values; and c) a scatterplot of OC3 versus EPA chl values. For each scatterplot  $r^2$  and RMSE values, as well as the line of best fit model equation are given. The line of best fit (solid line) and one-to-one line (dashed line) are shown on the scatterplots. Note that the vertical scales on the scatterplots are not all the same.

situ values, the RMSE in  $\mu\text{g/L}$  and the same data for the OC3 algorithm ( $r^2$  and RMSE). Also provided in the table are the EPA in situ chlorophyll mean and standard deviations for each lake as well as the modeled (CPA-A and OC3) chlorophyll mean and standard deviations. The model lines of best fit equations (slope and intercept) are also provided for both CPA-A and OC3 with respect to EPA in situ measurements. Most of the locations used in the evaluation were open lake sites where EPA conducts its standard cruises. The CPA-A  $r^2$  values using the lake specific HO models are 0.49 (Superior), 0.78 (Michigan), 0.69 (Huron), 0.55 (Erie), and 0.08 (Ontario). The RMSE in  $\mu\text{g/L}$  varied from a low value of 0.13 for Huron to a high value of 2.18 for Erie. For these open lake comparisons, the OC3 also performed well, with the exception of Lake Erie, generating  $r^2$  of 0.45 (Superior), 0.74 (Michigan), 0.71 (Huron), 0.20 (Erie), and 0.04 (Ontario). The OC3 RMSE values were also acceptable with the exception of Lake Erie (9.11). The relatively poor performance of the OC3 chl retrieval in Lake Erie is not surprising since the majority of Lake Erie water is Case II.

To address the question of the need for individual HO models for each lake, an average HO set of coefficients was generated by averaging the individual lake values. Table 4 is the result of using an all Great Lakes HO model in CPA-A retrievals. The table again presents the lake, number of EPA sites used and the  $r^2$  and RMSE as well as the modeled chlorophyll mean and standard deviation for each lake. Also provided is the CPA-A model line of best fit equation with respect to EPA chlorophyll in situ observations. The  $r^2$  values ranged from 0.03 to 0.43, with a low and high RMSE values of 0.04 and .94 respectively. Comparison of the CPA-A  $r^2$  values presented in Tables 3 and 4 clearly indicates that better results were obtained for all five Great Lakes when individual lake HO models were used. For Lake Ontario the use of a composite all lake HO model produced similar results as the individual Lake Ontario

HO model. This result is not particularly surprising for Lake Ontario that exhibits dramatic changes in water quality throughout the vegetative season. The original Bukata HO model based on in situ measurements only from Lake Ontario was also evaluated on all lakes as was done with the composite HO model, resulting in very poor retrievals ( $r^2$  of <0.30).

Representative CPA-A retrievals of chl, doc, and sm for all five lakes will now be presented, along with the OC3 outputs as well as statistics on the accuracy of the retrievals. Locations of the sampling sites are shown on several of the figures and help address the question of algorithm performance in Case II waters of the Great Lakes. Fig. 3 gives the new Lake Michigan CPA-A applied to a 1 km spatial resolution MODIS image collected on August 8, 2010. The MODIS bands used in the CPA-A have a spatial resolution of 1 km. Shown in the figure are the concentrations for chl, doc, and sm. A legend is provided indicating concentration levels for each of the CPA-A constituents. Hatched areas in the figure indicate no retrieval information, which is a result of clouds, poor atmospheric correction (i.e. negative radiance), or significant lake bottom return in optically shallow water. Note that for this August image the sm values are very low in the cloud free portion of the lake, and doc levels are higher on the western and northern areas. While the open lake values are very low the CPA-A is capable of tracking the sm gradient throughout the lakes albeit with uncertain absolute concentration accuracy (Shuchman et al., 2006). The analysis of sm particle size and scattering properties in the Great Lakes is ongoing and will certainly yield more robust estimates of sm backscatter thus improving the performance of the CPA-A with respect to sm concentration estimates.

Fig. 4 compares the CPA-A chl map to the standard OC3 chl retrieval for the same MODIS image collected on August 8, 2010. The OC3 algorithm was selected for comparison because this is the default chl model

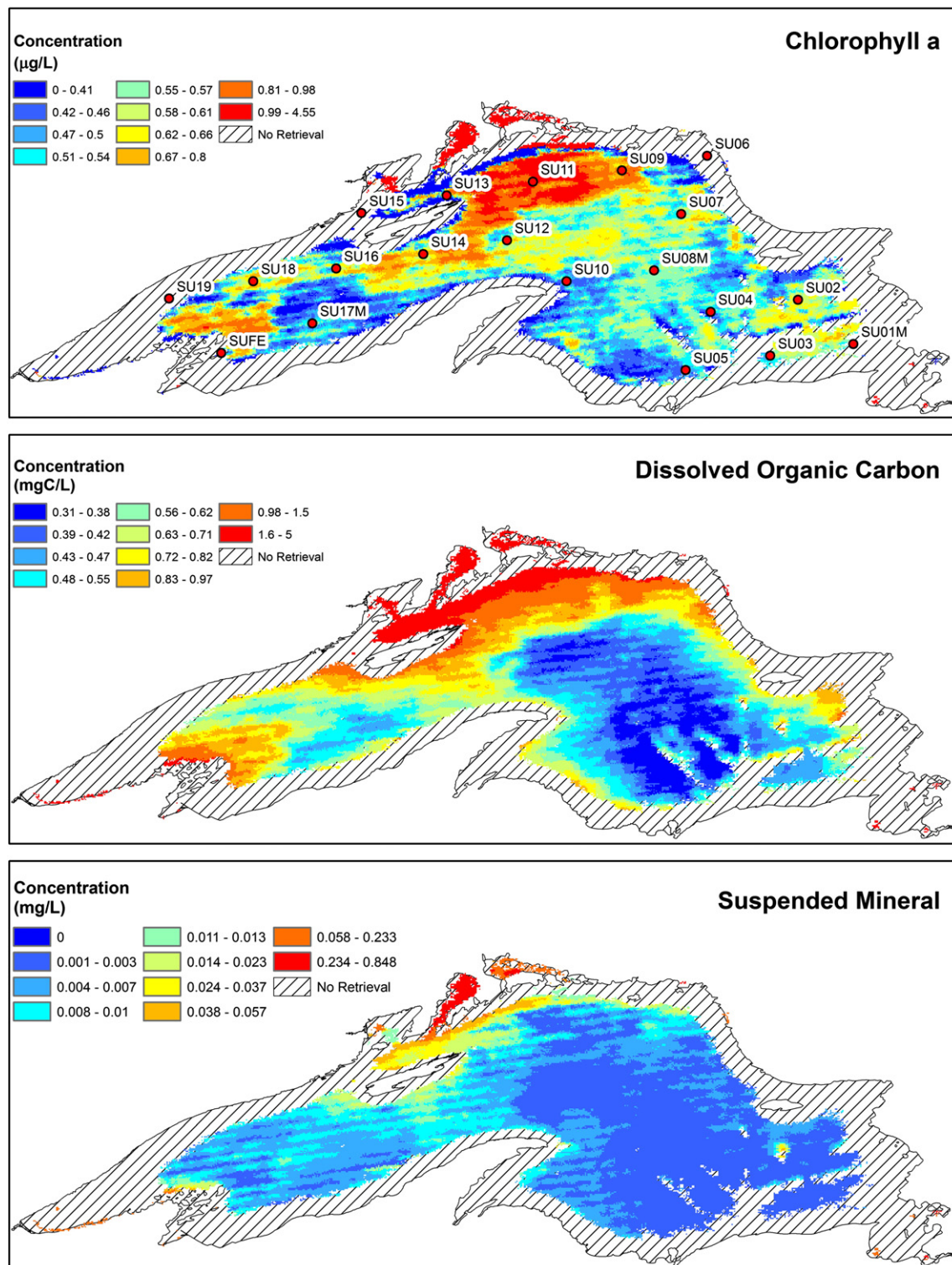


**Fig. 8.** Lake Superior CPA-A retrieval for August 25, 2008 MODIS image. Note the higher chl and doc values on the northern shoreline and the very low sm values through the entire lake which is consistent with in situ observations. In this case the hatched areas are locations of optically shallow water and/or cloud cover where the present CPA-A will not generate retrievals. The legends next to each map indicate the concentrations. The red dots indicate the EPA sampling station locations.

distributed by NASA. The EPA stations from a cruise (August 2 to August 5, 2010) are shown as red dots on the images. This August 8, 2008 image was the closest cloud free observation corresponding to the cruise dates. Examination of the OC3 and CPA-A chl retrievals in the open portion of the lake indicates slightly lower chl values produced by the OC3 algorithm when compared to the CPA-A estimates.

Fig. 5 compares the EPA in situ chl values (red dots in Fig. 3) to the CPA-A and OC3 derived estimates for the standard field campaign years 2010 and 2011. Presented in the fig. is a) a bar chart of CPA-A, OC3, and EPA chl concentrations at each station; b) a scatterplot of CPA-A versus EPA chl values; and c) a scatterplot of OC3 versus EPA chl values. Fig. 5a confirms the visual observations in Fig. 4, namely

the OC3 produces chl estimates that are on the average lower than the EPA in situ observations. The scatterplot shown in Fig. 5b produced an  $r^2$  of 0.78 and a resulting RMSE of 0.27 and indicates good agreement at both low and high chl concentrations for this limited dataset. The OC3 results (Fig. 5c) are also good producing an  $r^2$  of 0.74 and an RMSE of 0.48. Note that the line of best fit (solid line) and the one-to-one line (dashed line) are shown on the scatterplots. It should also be noted that the inherent bias visible in the OC3 retrievals (Fig. 5a) is not reflected in the RMSE but can be observed in the large negative intercept ( $-0.81$ ) and steep positive slope (1.99) of the best fit line.

A large box (see red outline in Fig. 4) was drawn around the 2010 EPA stations to compare the average chl value for this portion of the lake. The EPA station average was  $0.66 \mu\text{g/L}$  versus  $0.69 \mu\text{g/L}$  for the CPA-A results and  $0.42 \mu\text{g/L}$  for the OC3 results. Accurate chl estimates are important input parameters into a Great Lakes primary productivity model (Shuchman et al. 2013 2013).

Fig. 6, an August 12, 2010 1 km resolution MODIS CPA-A retrieval, represents typical results for Lake Huron. The new CPA-A with a specific HO model for Lake Huron performs well as shown in the figure. Note how the algorithm captures the higher values of chl, doc, and sm in the vicinity of Saginaw Bay. The red dots shown on the chl retrieval in the figure represent the EPA sampling stations used in the evaluation. These station locations were the same for both years.

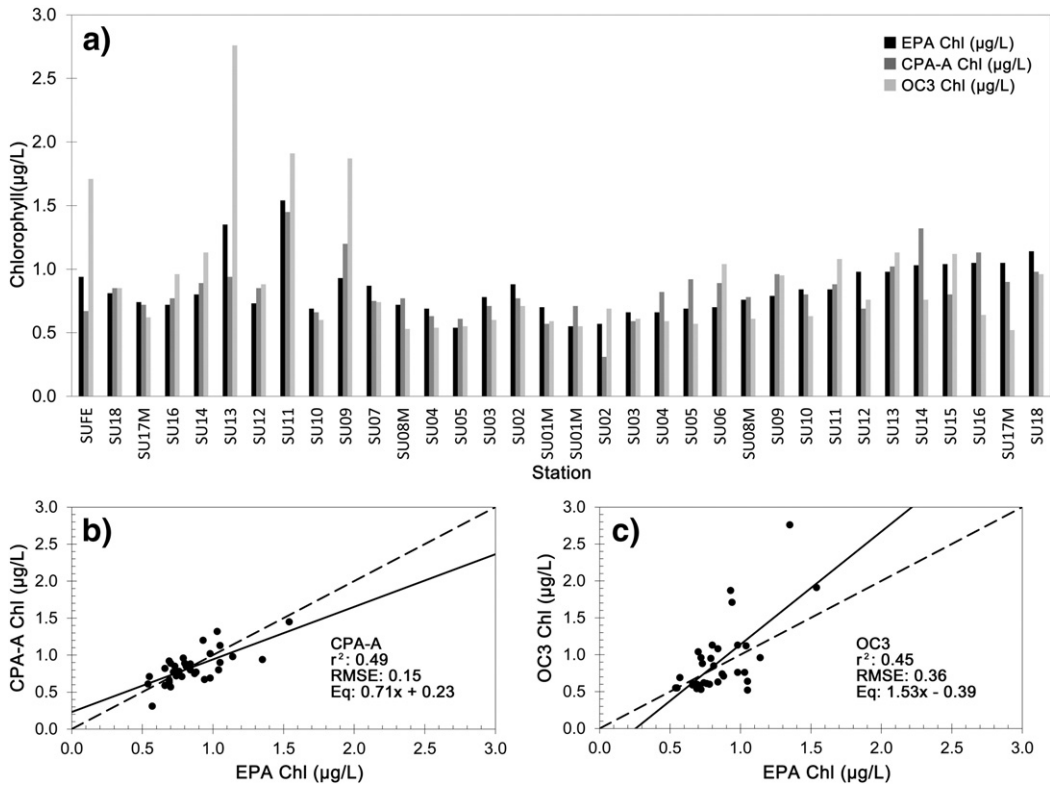
Fig. 7 is similar to Fig. 5 and shows a) a bar chart of CPA-A, OC3, and EPA chl concentrations at each station; b) a scatterplot of CPA-A versus EPA chl values; and c) a scatterplot of OC3 versus EPA chl values. Examination of the bar chart (2010 and 2011) indicates a similar conclusion as observed in Lake Michigan, namely the CPA-A and OC3 both performed well, not a surprise due to the similarities in the IOPs between the two lakes (O'Donnell et al. 2010). Note from Fig. (7b) that the CPA-A generated an  $r^2$  of 0.69 and RMSE of 0.13, while the OC3 (Fig. 7c) produced an  $r^2$  of 0.71 and RMSE of 0.19. Note the very good fit produced by the CPA-A

relative to the one-to-one line (slope 0.96, intercept 0.03). The OC3 values are slightly low biased as observed by the negative equation intercept, again similar to the Lake Michigan case.

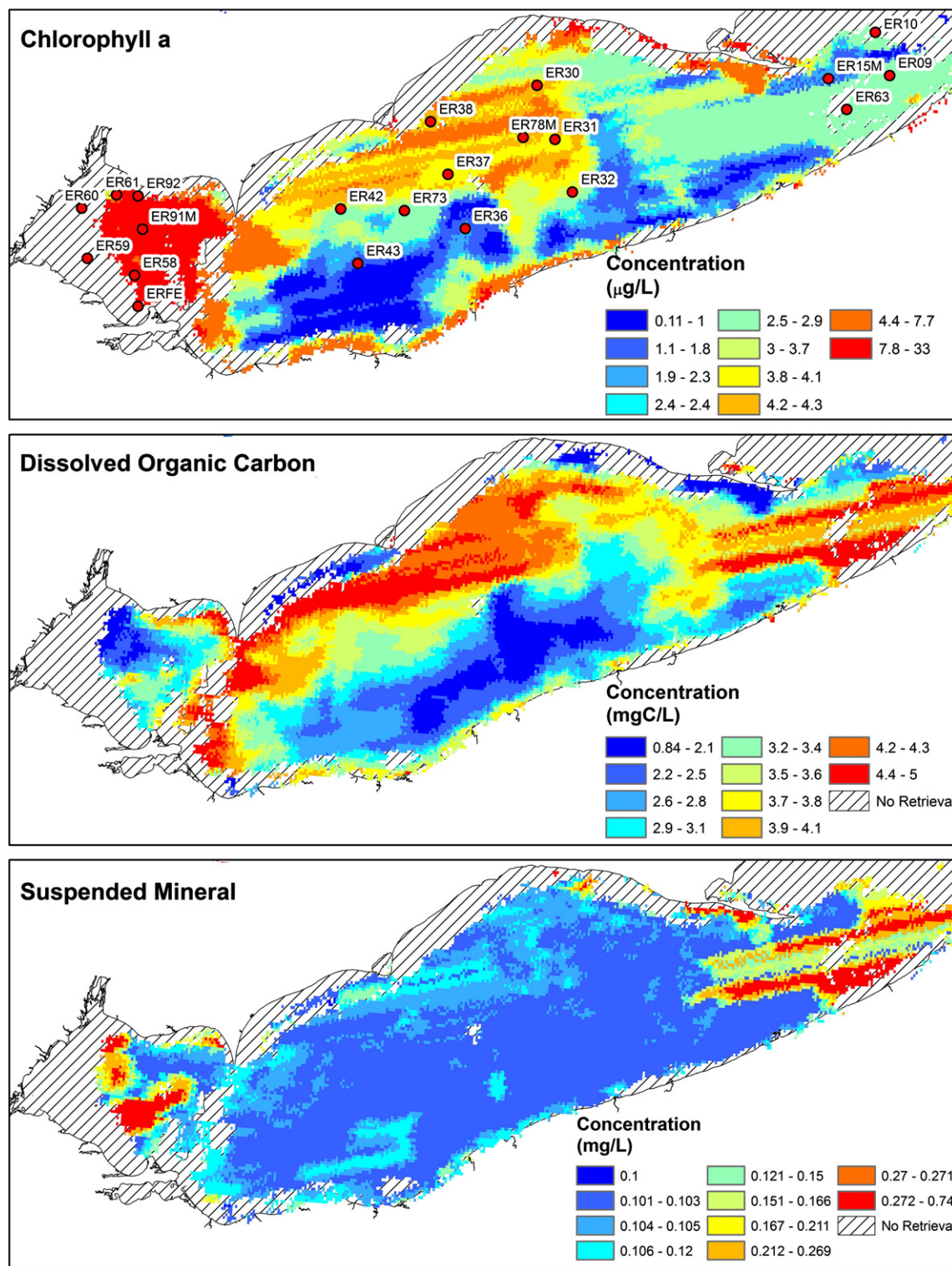
An example of Lake Superior CPA-A retrieval for August 25, 2008 is presented in Fig. 8. The variations in chl concentrations are visible on the CPA-A chl map as well as indicating the very low values of doc and sm except in localized near shore areas that have river input of the two constituents. The red dots in the figure again indicate the standard EPA field campaign locations that are used in their yearly lake surveys.

Fig. 9 again shows a) a bar chart of CPA-A, OC3, and EPA chl concentrations at each station; b) a scatterplot of CPA-A versus EPA chl values; and c) a scatterplot of OC3 versus EPA chl values. In this case the bar chart, which includes observations from 2008 to 2011, indicates the OC3 over estimated chl concentrations in near shore areas of Lake Superior where more than just chl was present. The CPA-A results were quite accurate both in the open lake where chl is the dominant CPA as well as in the near shore areas that can be classified as Case II water. The CPA-A  $r^2$  of 0.49 with and RMSE of  $0.15 \mu\text{g/L}$  (Fig. 9b) versus the OC3  $r^2$  of 0.45 and RMSE of  $0.36 \mu\text{g/L}$  substantiate the qualitative observation from the bar chart.

Fig. 10 is a representative CPA-A retrieval for Lake Erie using a MODIS image collected on August 7, 2010. Note the Lake Erie case has higher concentration values in respect to the other lakes as indicated on each map legend. The EPA field campaign stations again are shown in red. The new CPA-A for Lake Erie appears to successfully capture the complexity and high chl values in the western basin which was indicative of a harmful algal bloom (HAB) event. The doc and sm maps also visible in the figure produced values that are spatially consistent with reported in situ observations (O'Donnell et al. 2010). Note the streaking in the eastern basin of the lake that is indicative of poor atmospheric correction due to cloud and haze contamination. Significant



**Fig. 9.** Comparison of the Lake Superior EPA in situ chl values to the CPA-A and OC3 derived estimates for the standard field campaign years of 2008 and 2011. Shown is a) a bar chart of CPA-A, OC3, and EPA chl concentrations at each station; b) a scatterplot of CPA-A versus EPA chl values; and c) a scatterplot of OC3 versus EPA chl values. For each scatterplot  $r^2$  and RMSE values, as well as the line of best fit model equation are given. The line of best fit (solid line) and one-to-one line (dashed line) are shown on the scatterplots. Note that the vertical scales on the scatterplots are not all the same.



**Fig. 10.** Lake Erie CPA-A retrieval for an August 7, 2010 MODIS image shows higher concentrations of the constituents than other lakes. The new Erie HO model appears to capture the complexity and higher values indicative of the water properties found in the Western Basin although the sm estimates throughout the lake appear lower than expected. The hatched areas again indicate no retrieval. The red dots again indicate the EPA sampling station locations.

amounts of doc can be observed in the north-central basin as well as significant sediment in the western basin on this August 7, retrieval. These doc and sm signals will affect the retrieval of the chl component as evident in the OC3 retrieval (site ER38). Validation of sm and doc absolute concentration retrievals for Lake Erie is ongoing as more in situ data is collected and made available.

Fig. 11, consistent with Figs. 5, 7, and 9, represents a) bar chart of CPA-A, OC3, and EPA chl concentrations at each station for the 2009 and 2010 field campaigns; b) scatterplot of CPA-A versus EPA chl values; and c) scatterplot of OC3 versus EPA chl values. In this case where literally all of Lake Erie is comprised of Case II water the CPA-A correctly estimates chl concentration producing an  $r^2$  of 0.55 with and RMSE of

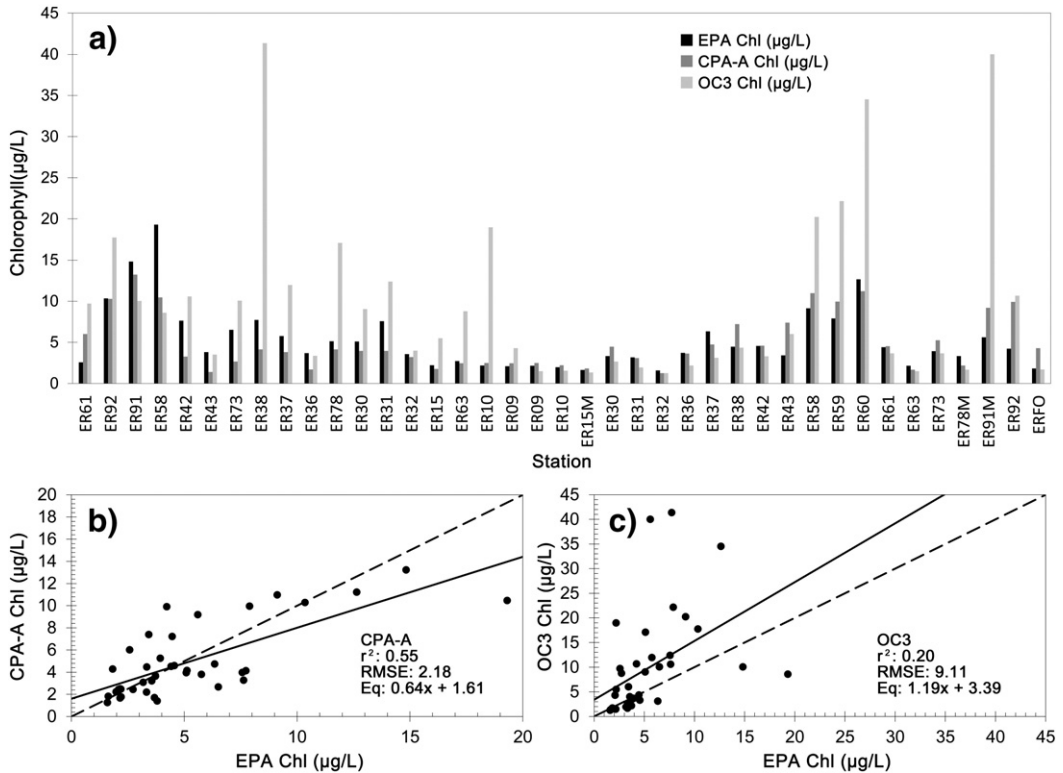


**Fig. 11.** Comparison of the Lake Erie EPA in situ chl values to the CPA-A and OC3 derived estimates for the standard field campaign years of 2009 and 2010. Shown in the figure is a) a bar chart of CPA-A, OC3, and EPA chl concentrations at each station; b) a scatterplot of CPA-A versus EPA chl values; and c) a scatterplot of OC3 versus EPA chl values. For each scatterplot  $r^2$  and RMSE values, as well as the line of best fit model equation are given. The line of best fit (solid line) and one-to-one line (dashed line) are shown on the scatterplots. Note that the vertical scales on the scatterplots are not all the same.

2.18. The OC3 over predicted the amount of chl in areas of the lake where significant quantities of doc and sm were present. The  $r^2$  of 0.20 and RMSE of 9.11 µg/L do not adequately portray the large errors and variability of chl in Lake Erie and therefore are not as useful in identifying potential HAB events (Fahnstiel personal communication).

A set of chl, doc, and sm maps for Lake Ontario are shown in Fig. 12 along with the standard EPA sampling stations. This particular August 6, 2008 overpass is interesting as it captured a whiting event. The whiting event is identified by the evaluated levels of the sm concentration which are represented by the brown colored area in the eastern basin on the sm map. Whiting events (O'Donnell et al., 2009) appear as large areas of high reflectivity (almost white in color from the air) the result of calcium carbonate being precipitated due to a water temperature increase. High sediment load is also observed in the western portion of Lake Ontario in the vicinity of the Niagara River. Note the low levels of doc in the whiting event as a result of scavenging of doc by sm (Shuchman et al., 2006). The CPA-A generated doc map values are again consistent with UFL observations.

In this case the CPA-A and OC3 produced similar results (see Fig. 13) with  $r^2$  of 0.08 and RMSE of 0.82 for the CPA-A and an  $r^2$  of 0.04 and RMSE of 0.83 for the OC3 when compared to the 2008 and 2011 field campaign data. Note that the  $r^2$  for the CPA-A for Lake Ontario is lower than the  $r^2$  for the other four lakes by a large margin. The reduced performance of the CPA-A in Lake Ontario can be attributed to several factors including: 1) the new Lake Ontario HO model is not fully optimized, perhaps a result of using the older Bukata chl and sm backscatter coefficients; 2) the lake exhibits large variability in CPA constituents in a given year, suggesting a single HO model is insufficient; and 3) the circulation dynamics in Lake Ontario are such that the five day difference between satellite overpass and field collection introduced errors in the evaluation.

The original Bukata HO model was also run on this August 2008 Lake Ontario data set to confirm the hypothesis that a new set of coefficients were necessary to optimize the CPA-A retrieval performance. The use of the original Bukata coefficients produces a less accurate retrieval with an  $r^2 < 0.04$  and an RMSE greater than 0.85.

In summary the comparisons between the CPA-A and OC3 chl concentration retrievals and the EPA in situ observations confirm the hypothesis that individual lake HO models are required to optimize chl estimates from satellites. Additionally, the band ratio OC3 algorithm generates acceptable chl concentration estimates in areas of the lakes where the dominant CPA is chl and the values are 5 µg/L or less. In areas of the Great Lakes where significant quantities of doc and sm exist as well as chl concentrations above approximately 5 µg/L a three color component algorithm such as the CPA-A is recommended to obtain more robust chl estimates.

#### Application of CPA-A to other remote sensing systems

The new CPA-A is not satellite sensor specific. The algorithm simply requires spectral bands of narrow range (e.g. 10 nm) and strategically placed centers within the portion of the electromagnetic spectrum (i.e. 412, 440, 490, 531, 547, 667 nm) that cover ocean color reflecting features (i.e. chl, sm, and cdom/doc). A number of satellite systems that are presently operating or soon to be launched (see Fig. 14) can be used to generate CPA-A concentration maps. In Fig. 14 the vertical lines indicate the bands presently used in the suite of Great lakes CPA algorithms. Of the six bands indicated a minimum of only three is required to obtain a successful retrieval, thus many of the systems presented (NIMBUS (CZCS), SeaWiFS, MERIS, and MODIS) can produce historical time series chl, doc, and sm concentrations dating back to 1979. VIIRS and the hyperspectral imager on the international space

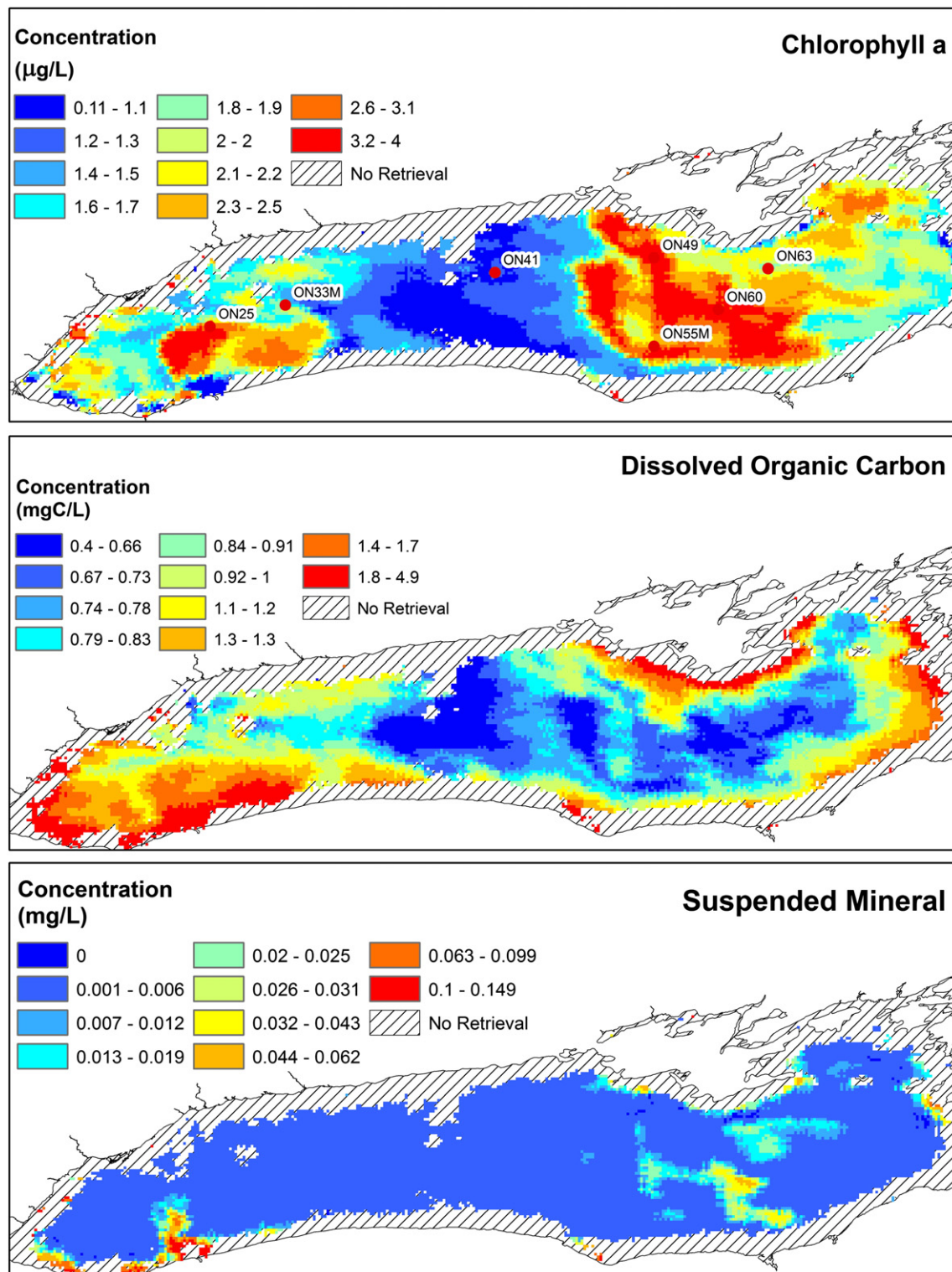


**Fig. 12.** CPA-A retrieval maps for an August 6, 2008 Lake Ontario image. This set of chl, doc, and sm maps shows the complexity of Lake Ontario and in this case captured a whiting event in the eastern portion of the lake indicated in brown on the sm map. The low levels of doc in the high sm area of the whiting event m of scavenging of doc by sm. The red dots indicate the EPA sampling station locations.

station (HICO) can be used to generate concentration values of chl, doc, and sm for the Great Lakes.

The launch of the new NPOESS Preparatory Project (NPP) with the VIIRS sensor, which has a spatial resolution of approximately 700 m and 22 bands (seven Ocean Color bands), will provide CPA-A retrievals comparable to those of MODIS and MERIS. It should be noted that the

ocean color sensing bands of VIIRS are on average 7 nm wider than MODIS, which will require HO parameters to be recalculated to represent the different band widths.

Fig. 15 is an example of the CPA-A applied to MERIS European Space Agency (ESA) satellite data collected over Lake Michigan. In this August 12, 2010 image, with a spatial resolution of approximately 330 m, finer

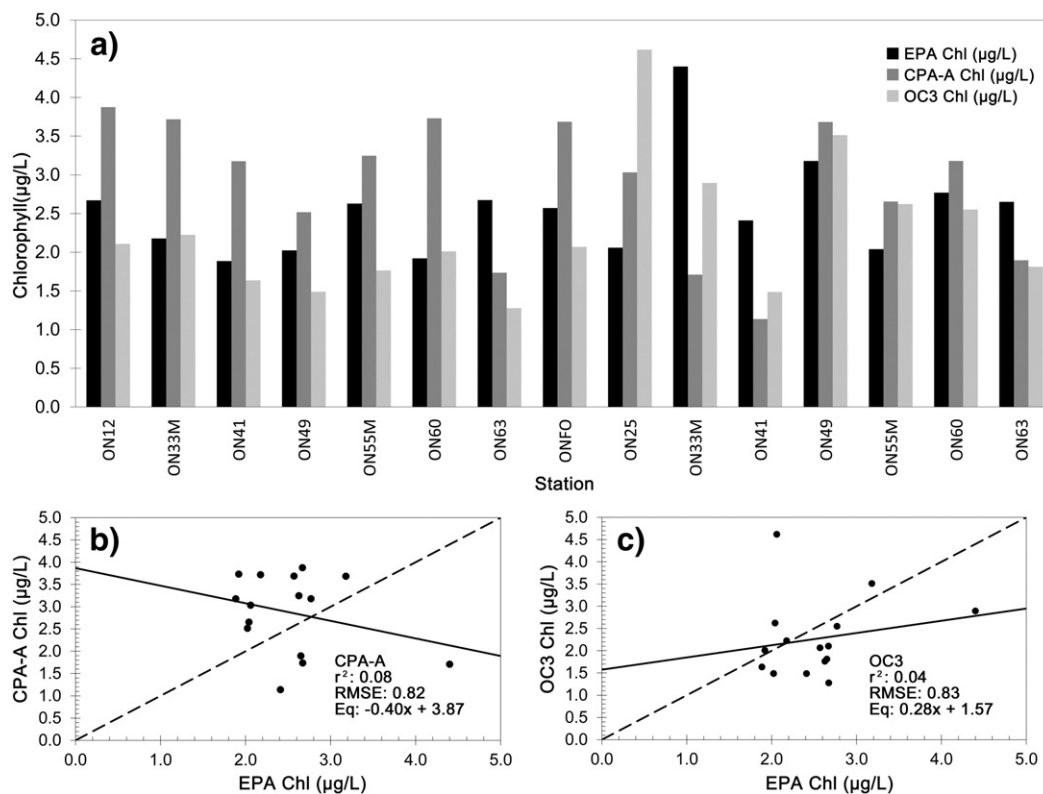


**Fig. 13.** Comparison of the Lake Ontario EPA in situ chl values to the CPA-A and OC3 derived estimates for the standard field campaign years 2008 and 2011. Shown in the figure is a) a bar chart of CPA-A, OC3, and EPA chl concentrations at each station; b) a scatterplot of CPA-A versus EPA chl values; and c) a scatterplot of OC3 versus EPA chl values. For each scatterplot  $r^2$  and RMSE values, as well as the line of best fit model equation are given. The line of best fit (solid line) and one-to-one line (dashed line) are shown on the scatterplots. Note that the vertical scales on the scatterplots are not all the same.

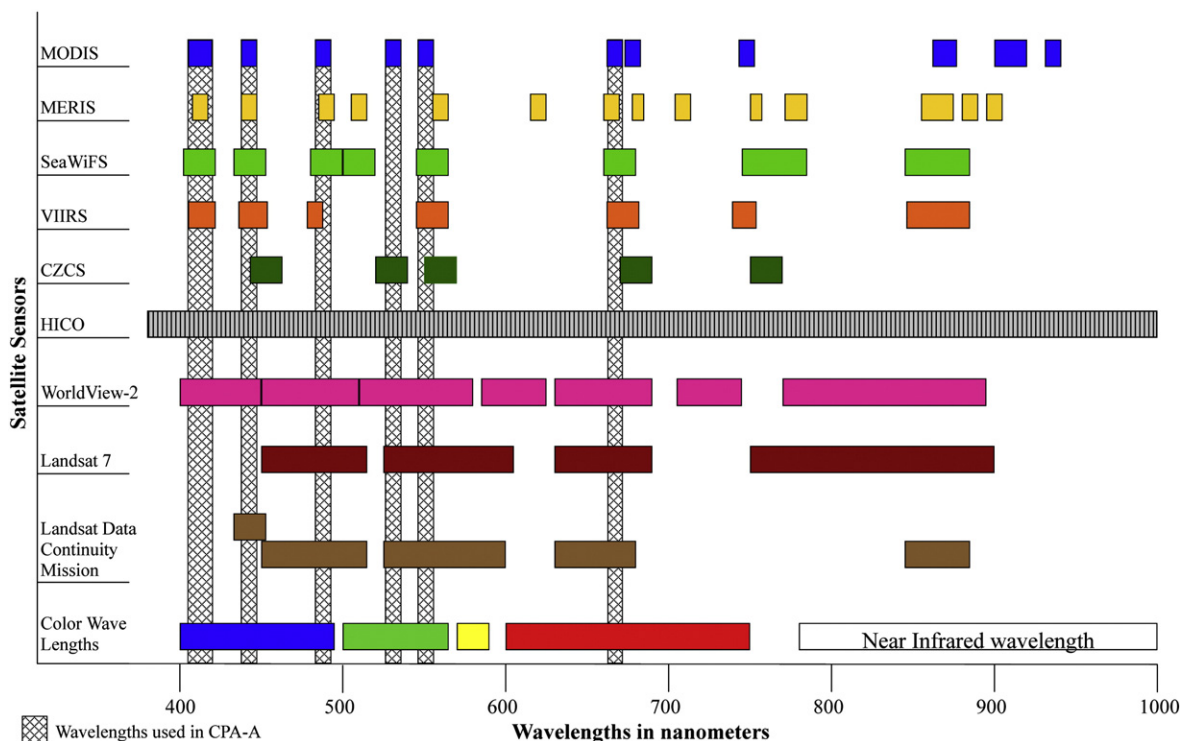


**Fig. 14.** Radiation spectral bands of various spaceborne sensors that operate in the visible and NIR portion of the electromagnetic spectrum that may be used for water quality applications. The vertical hatched bars indicate bands that are presently used in the new suite of CPA-A Great Lakes algorithms. The algorithms perform well using a minimum of three of the six bands indicated in the figure.

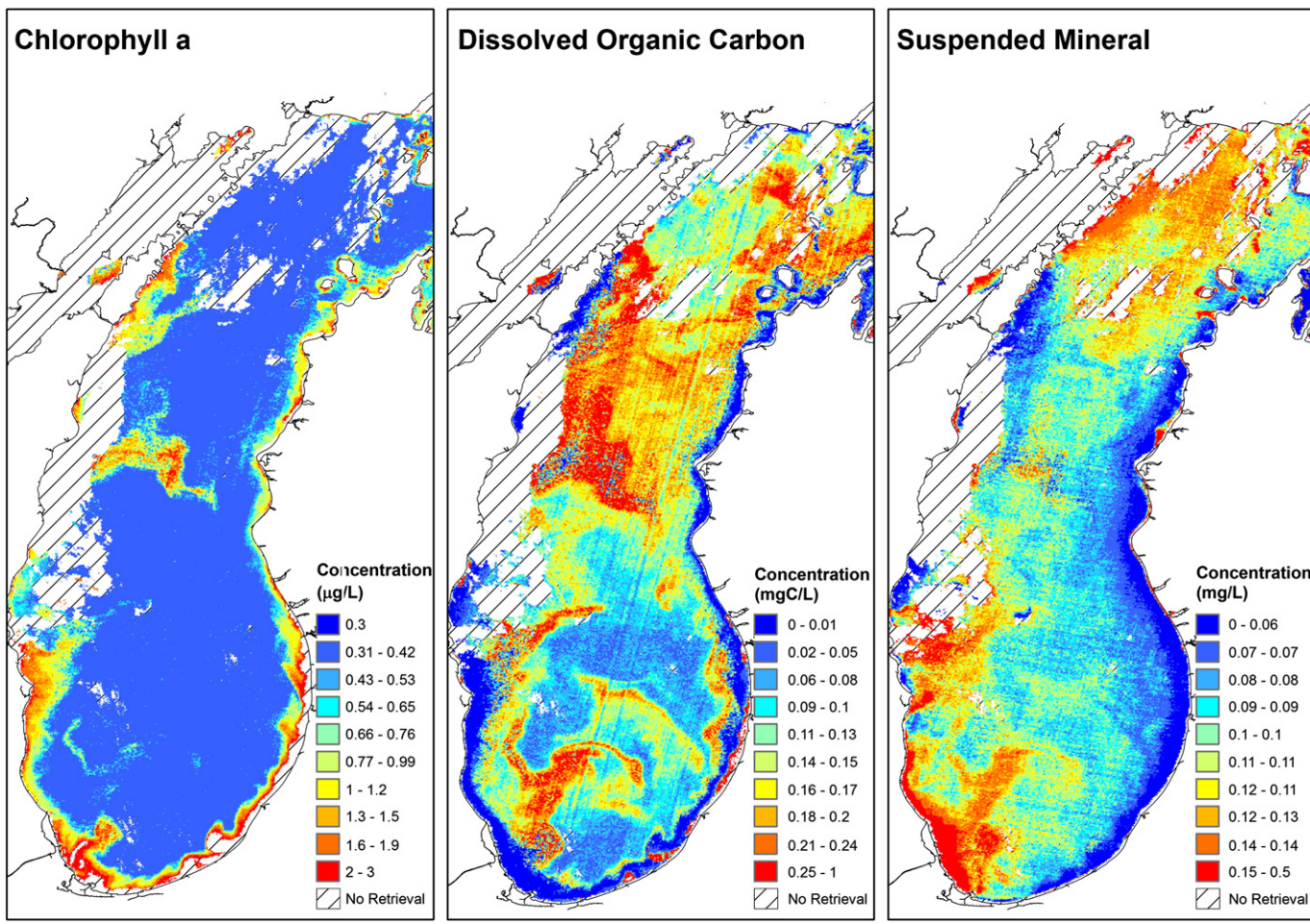


**Fig. 15.** August 12, 2010 MERIS CPA-A retrieval for Lake Michigan showing the finer detailed CPA concentrations made possible by the 330 meter resolution pixels. Narrow bands of higher (e.g. chl on western side of Lake Michigan) and lower (chl along eastern shore) concentrations of chl, doc, and sm along the near shore are visible. The MERIS retrievals are similar to those obtained from the MODIS images collected two days earlier (Fig. 2).

detail in the chl, doc, and sm concentration maps can be observed. Note the higher chl values along the Lake Michigan shore as well as the large bloom half way up the lake. On the doc retrieval the values are low except in the vicinity of river mouths, the source of this CPA. The sm concentration is relatively low throughout the lake with the exception of a re-suspension event in the vicinity of Chicago. The chl retrieval from this MERIS dataset was evaluated in respect to EPA in situ observations collected within 7 days of the overpass. An  $r^2$  of 0.97 with a RMSE of 0.05  $\mu\text{g/L}$  resulted when comparing a 3-by-3 pixel average with the 2010 EPA field campaign data. These results are very similar to those obtained from the MODIS image collected on August 8, 2010.

### Concluding remarks

A comprehensive set of IOP measurements with corresponding in situ measurements of chl, doc, cdom, sm, and TSS have been assembled into a database for all the Great Lakes. These data will be available via an interactive geospatial web portal in 2013. This data set developed over several years of research cruises indicated the need for separate HO models for each of the Great Lakes to obtain the required retrieval concentration accuracies. This database that spans nearly two decades of observations also provides insight into how the optical properties of the Great Lakes have changed due to invasive species introduction, anthropogenic and climate change forcing.

The new HO models for all five lakes are quite robust, with the estimates of chl comparing favorably to the near coincident EPA chl values.

The doc and sm derived values provided simultaneously during the retrieval process track the respective concentration gradients throughout the lakes. Absolute accuracy of the two CPAs will continue to be evaluated as more in situ data becomes available. The Lake Erie CPA-A estimates of chl, doc, and sm are robust enough to be used to generate harmful algae blooms (HABs) advisory maps for the EPA (Shuchman et al., 2012). The HAB mapping algorithm employed by MTRI uses an empirically derived relationship between high values of chlorophyll and Cyanobacteria (Fahnenstiel et al., 2008; Millie et al., 2011; Stumpf et al., 2012). The Lake Ontario CPA-A chl concentration values, which produced the lowest  $r^2$  value when compared to EPA observations, reveal the complexity of this lake with low chl values reported by the EPA of approximately 1  $\mu\text{g/L}$  in the spring to values of 4.5  $\mu\text{g/L}$  in the late summer.

The limited comparisons presented between the CPA-A and OC3 chl concentration retrievals and the EPA in situ observations demonstrated that individual lake HO models are required to optimize chl estimates from satellites. The OC3 algorithm that utilizes a band ratio approach (O'Reilly et al. 2000b) generates acceptable chl concentration estimates in areas of the Great Lakes where the dominant CPA is chl and the values are 5  $\mu\text{g/L}$  or less. In areas of the Great Lakes where significant quantities of doc and sm exist as well as chl concentrations above approximately 5  $\mu\text{g/L}$ , such as Lake Erie, a three color component algorithm such as the CPA-A is required to obtain robust chl estimates.

The atmospheric correction investigation was quite illuminating. The analysis confirmed the supposition that in the open areas of the

lakes, 20 km or greater from shore, the default iterative NIR correction (waves, glint, and aerosols) will do an acceptable job. However, contrary to popular belief that in Case II near shore water and literally all of Lake Erie a more sophisticated atmospheric correction approach would be required, this analysis indicated that for all the Great Lakes, the default iterative NIR atmospheric correction is adequate thus allowing a user to use the standard product. Tuning of a fixed model pair NIR iterative or fixed model pair atmospheric corrections may potentially improve retrievals in the western basin of Erie and in AOC areas; however, more research is needed.

## Acknowledgments

This investigation was supported by NASA Roses Grant # NNX09AU88G. The NASA technical monitor is Dr. Jared Entin. The development of the CPA-A code was supported under a GLOS Remote Sensing Grant Award NA070AR4320006 (CRDA no. 11.432, CILER under contract # 3001278616). Drs. Jennifer Read and Thomas Johengen were the GLOS and CILER technical monitors. We would like to thank Nathaniel Jesse, MTRI research assistant, and William Papineau, MTRI student intern, for the support they provided in analyzing the satellite data and acquiring the EPA in situ measurements. We would also like to thank three anonymous reviewers for their insightful comments and feedback. This is Contribution No. 85 of the Michigan Tech Research Institute (MTRI) at Michigan Technological University.

## References

- Ackleson, S., 2001. Ocean optics research at the start of the 21st century. *Oceanography* 14 (3), 5–8.
- Barbiero, R.P., Tuchman, M.L., Millard, S., 2006. Post-dreissenid increases in transparency during summer stratification in the offshore waters of Lake Ontario: is a reduction in whiting events the cause? *J. Great Lakes Res.* 32 (1), 131–141.
- Bergmann, T., Fahnstiel, G., Lohrenz, S., Millie, D., Schofield, O., 2004. The impacts of a recurrent resuspension event and variable phytoplankton community composition on remote sensing reflectance. *J. Geophys. Res. Oceans* 109. <http://dx.doi.org/10.1029/2002JC001575>.
- Binding, C.E., Jerome, J.H., Bukata, R.P., Booty, W.G., 2008. Spectral absorption properties of dissolved and particulate matter in Lake Erie. *Remote. Sens. Environ.* 112, 1702–1711.
- Binding, C.E., Greenberg, T., Bukata, R.P., 2012. An analysis of MODIS-derived algal and mineral turbidity in Lake Erie. *J. Great Lakes Res.* 38 (1), 10.
- Boyer, G.L., 2008. Cyanobacterial toxins in New York and the Lower Great Lakes ecosystems. In: Hudnell, H.K. (Ed.), *Cyanobacterial Harmful Algal Blooms: State of the Science and Research Needs, Advances in Experimental Medicine and Biology*. Springer, New York, New York, pp. 153–166.
- Budd, J.W., Warrington, D.S., 2004. Satellite-based sediment and chlorophyll a estimates for Lake Superior. *J. Great Lakes Res.* 30, 459–466.
- Bukata, R.P., Bruton, J.E., Jerome, J.H., 1983. Use of chromaticity in remote measurements of water quality. *Remote. Sens. Environ.* 13, 161–177.
- Bukata, R.P., Bruton, J.E., Jerome, J.H., 1985. Application of direct measurements of optical parameters to the estimation of lake water quality indicators. Scientific Series, 140. Inland Waters Directorate, National Water Research Institute, Canada Centre for Inland Waters, Burlington, Ontario, Canada.
- Bukata, R.P., Jerome, J.H., Kondratyev, K.Y., Pozdnyakov, D.V., 1995. *Optical Properties and Remote Sensing of Inland and Coastal Waters*. CRC Press, Boca Raton, Florida.
- D'Sa, E.J., Hu, C., Muller-Karger, F.E., Carder, K.L., 2002. Estimation of colored dissolved organic matter and salinity fields in case 2 waters using SeaWiFS: examples from Florida Bay and Florida Shelf. *Proceedings of the Indian Academy of Sciences. Earth Planet. Sci.* 111, 197–207.
- Effler, S.W., Perkins, M., Peng, F., Strait, C., Weidemann, A.D., Auer, M.T., 2010. Light-absorbing components in Lake Superior. *J. Great Lakes Res.* 36, 656–665.
- Fahnstiel, G.L., Millie, D.F., Dyble, J., Litaker, R.W., Tester, P.A., McCormick, M.J., Rediske, R., Klarer, D., 2008. Microcystin concentrations and cell quotas in Saginaw Bay, Lake Huron. *Aquat. Ecosyst. Heal. Manag.* 11 (2), 190–195.
- Fahnstiel, G.L., Nalep, T., Pothoven, S., Carrick, H., Scavia, D., 2010a. Lake Michigan lower food web: long-term observations and *Dreissena* impact. *J. Great Lakes Res.* 36 (3), 1–4.
- Fahnstiel, G.L., Pothoven, S., Vanderploeg, H., Klarer, D., Nelapa, T., Scavia, D., 2010b. Recent changes in primary productivity and phytoplankton in the offshore region of southeastern Lake Michigan. *J. Great Lakes Res.* 36 (3), 20–29.
- Gordon, H.R., Clark, D.K., 1981. Clear water radiances for atmospheric correction of coastal zone color scanner imagery. *Appl. Opt.* 24, 4175–4180.
- Gordon, H.R., Wang, M., 1994. Retrieval of water-leaving radiance and aerosol optical thickness over the oceans with SeaWiFS: a preliminary algorithm. *Appl. Opt.* 33, 443–452. <http://oceancolor.gsfc.nasa.gov>. <http://www.gdal.org/>.
- Jerlov, N.G., 1976. *Marine optics*. Elsevier Oceanography Series, 14. Elsevier Publ. Co., Amsterdam, The Netherlands.
- Jerome, J.H., Bukata, R.P., Miller, J.R., 1996. Remote sensing reflectance and its relationship to optical properties of natural waters. *Int. J. Remote. Sens.* 17 (16), 3135–3155.
- Kerfoot, W.C., Budd, J.W., Green, S.A., Cotner, J.B., Biddanda, B.A., Schwab, D.J., Vanderploeg, H.A., 2008. Doughnut in the desert: late-winter production pulse in southern Lake Michigan. *Limnol. Oceanogr.* 53 (2), 589–604.
- Korosov, A.A., Pozdnyakov, D.V., Folkestad, A., Pettersson, L.H., Sørensen, K., Shuchman, R., 2009. Semi-empirical algorithm for the retrieval of ecology-relevant water constituents in various aquatic environments. *Algoritm.* 2 (1), 470–497.
- Lampman, G.G., Makarewicz, J.C., 1999. The phytoplankton zooplankton link in the Lake Ontario food web. *J. Great Lakes Res.* 25, 239–249.
- Land, P.E., Haigh, J.D., 1997. Atmospheric correction over Case II waters using an iterative fitting algorithm including relative humidity. *SPIE* 2963, 609–612.
- Lee, Z., Carder, K.L., Chen, R.F., Peacock, T.G., 2001. Properties of the water column and bottom derived from Airborne Visible Infrared Imaging Spectrometer (AVIRIS) data. *J. Geo. Res.* 106, 11639–11651.
- Lesht, B.M., Barbiero, R.P., Warren, G.J., 2012. Satellite ocean color algorithms: a review of applications to the Great Lakes. *J. Great Lakes Res.* 38 (1), 49–60.
- Lesht, B.M., Barbiero, R.P., Warren, G.J., 2013. A band-ratio algorithm for retrieving open-lake chlorophyll values from satellite observations of the Great Lakes. *J. Great Lakes Res.* 39 (1), 138–152.
- Levenberg, K., 1944. A method for the solution of certain non-linear problems in least squares. *Quant. Appl. Math.* 2, 164–168.
- Lohrenz, S.E., Fahnstiel, G.L., Kirkpatrick, G.J., Carroll, C.L., Kelly, K.A., 1999. Microphotometric assessment of spectral absorption and its potential application for characterization of harmful algal species. *J. Phycol.* 35, 1438–1446.
- Lohrenz, S.E., Fahnstiel, G.L., Millie, D.F., Schofield, O.M.E., Johengen, T., Bergman, T., 2004. Spring phytoplankton photosynthesis, growth, and primary production and relationships to a recurrent coastal sediment plume and river inputs in southeastern Lake Michigan. *J. Geophys. Res.* 109, C10S14.
- Lohrenz, S., Fahnstiel, G., Schofield, O., Millie, D., 2008. Coastal sediment dynamics and river discharge as key factors influencing coastal ecosystem productivity in southeastern Lake Michigan. *Oceanography* 21 (4), 6169.
- Marquardt, D.W., 1963. An algorithm for least-squares estimation of nonlinear parameters. *J. Int. Soc. Appl. Math.* 11 (2), 36–48.
- Millie, D.F., Fahnstiel, G.L., Weckman, G.R., Klarer, D.M., Bressie, D., Vanderploeg, H.A., Fishman, D.B., 2011. An “enviro-informatic” assessment of Saginaw Bay (Lake Huron, USA) phytoplankton: data driven characterization and modeling of microcysts (Cyanophyta). *J. Phycol.* 47, 714–730.
- Morel, A., Briand, A., 1986. Inherent optical properties of algal cells including picoplankton: theoretical and experimental results. In: Platt, T., Li, W.K.W. (Eds.), *Photosynthetic picoplankton*. Canadian Bulletin of Fisheries and Aquatic Sciences, 214, pp. 521–559.
- Morel, A., Prieur, L., 1977. Analysis of variation in ocean colour. *Limnol. Oceanogr.* 22 (4), 709–722.
- Mortimer, C.H., 1988. Discoveries and testable hypotheses arising from coastal zone color scanner imagery of southern Lake Michigan. *Limnol. Oceanogr.* 33 (2), 203–226.
- Nalepa, T.F., Fanslow, D.L., Land, G.A., 2009. Transformation of the offshore benthic community in Lake Michigan: recent shift from the native amphipod *Diporeia* spp. to the invasive mussel *Dreissena rostriformis bugensis*. *Freshw. Biol.* 54, 466–479.
- O'Donnell, D.M., Quaring, G.F., Strait, C.M., Effler, S.W., Leshkevich, G.A., 2009. Spectral measurements of absorption, beam attenuation and backscattering coefficients, and remote sensing reflectance in four Laurentian Great Lakes. 52nd annual conference on Great Lakes Research. Lecture conducted for IAGLR on May 20. (Toledo, Ohio).
- O'Donnell, D.M., Effler, S.W., Strait, C.M., Leshkevich, G.A., 2010. Optical characterizations and pursuit of optical closure for the western basin of Lake Erie through in situ measurements. *J. Great Lakes Res.* 36 (1), 736–746.
- O'Reilly, J.E., Maritorena, S., Mitchell, G., Siegel, M.A., Carder, K.L., Garver, S.A., Kahru, M., McClain, C., 1998. Ocean color chlorophyll algorithms for SeaWiFS. *J. Geophys. Res.* 103 (11), 24937–24953.
- O'Reilly, J., Maritorena, S., O'Brien, M., Siegel, D., Toole, D., Menzies, D., Smith, R., Mueller, J., Mitchell, B., Kahru, M., Chavez, F.P., Strutton, P., Cota, G., Hooker, S., McClain, C., Carder, K., Müller-Karger, F., Harding, L., Magnuson, A., Phinney, D., Moore, G., Aiken, J., Arrigo, K., Letelier, R., Culver, M., 2000a. *SeaWiFS Postlaunch Calibration and Validation Technical Report Series. SeaWiFS Postlaunch Calibration and Validation Analyses, Part 3*, NASA Technical Memorandum, 11.
- O'Reilly, J., Maritorena, S., Siegal, D., O'Brien, M., Toole, D., Chaves, F., Strutton, P., Cota, G., Hooker, S., McClain, C., Carder, K., Müller-Karger, F., Harding, L., Magnuson, A., Phinney, D., Moore, G., Aiken, J., Arrigo, K., Letelier, R., Culver, M., 2000b. *SeaWiFS postlaunch calibration and validation analyses, Part 3*. In: Hooker, S.B., Firestone, E.R. (Eds.), *NASA Technical Memorandum 206892*. NASA, Goddard Space Flight Center, 11. Greenbelt, Maryland, pp. 9–24.
- Peng, F., Effler, S.W., 2011. Characterizations of the light-scattering attributes of mineral particles in Lake Ontario and the effects of whiting. *J. Great Lakes Res.* 37 (4), 672–682.
- Peng, F., Effler, S.W., O'Donnell, D.M., Weidemann, A.D., Auer, M.T., 2009. Characterization of mineralogenic particles in support of modeling light scattering in Lake Superior through a two-component approach. *Limnol. Oceanogr.* 54 (4), 1369–1381.
- Pozdnyakov, D., Grassl, H., 2003. *Colour of Inland and Coastal Waters: A Methodology for Its Interpretation*. Springer-Praxis, Chichester, U.K.
- Pozdnyakov, D., Bakan, S., Grassl, H., 2000a. *Atmospheric Correction of Colour Images in Case I Waters – A Review, Report No. 308*. Max-Planck Institute for Meteorology, Germany.
- Pozdnyakov, D., Bakan, S., Grassl, H., 2000b. *Atmospheric Correction of Colour Images of Case II Waters – A Review*. Report No. 308. Max-Planck Institute for Meteorology, Germany.
- Pozdnyakov, D., Shuchman, R., Korosov, A., Hatt, C., 2005. Operational algorithm for the retrieval of water quality in the Great Lakes. *Remote. Sens. Environ.* 97, 353–370.

- Rinta-Kanto, J.M., Oullette, A.J.A., Twiss, M.R., Boyer, G.L., Bridgeman, T.B., Wilhelm, S.W., 2005. Quantification of toxic *Microcystis* spp. during the 2003 and 2004 blooms in western Lake Erie using quantitative real-time PCR. Environ. Sci. Technol. 39, 4198–4205.
- Ruddick, K.G., Ovidio, F., Rijkeboer, M., 2000. Atmospheric correction of SeaWiFS imagery for turbid coastal and inland waters. Appl. Opt. 39 (6), 897–912.
- Shuchman, R., Korosov, A., Hatt, C., Pozdnyakov, D., 2006. Verification and application of a bio-optical algorithm for Lake Michigan using SeaWiFS: a 7-year inter-annual analysis. J. Great Lakes Res. 32, 258–279.
- Shuchman, R., Sayers, M., Brooks, C., Fahnenstiel, G., Leshkevich, G., 2012. Mapping harmful algae blooms (HABs) in the Great Lakes using MODIS and MERIS satellite data. 55th Annual Conference of the International Association for Great Lakes Research. Lecture conducted for IAGLR — Cornwall, Ontario.
- Shuchman, R., Sayers, M., Fahnenstiel, G., Leshkevich, G., 2013. A model for determining satellite-derived primary productivity estimates for Lake Michigan. J. Great Lakes Res. 39, 46–54.
- Siegel, D.A., Wang, M., Maritorena, S., Robinson, W., 2000. Atmospheric correction of satellite ocean color imagery: the black pixel assumption. Appl. Opt. 39 (21), 3582–3591.
- Speziale, B.J., Schreiner, S.P., Giannatteo, P.A., Schindler, J.E., 1984. Comparison of N,N-dimethylformamide, dimethyl sulfoxide, and acetone for extraction of phytoplankton chlorophyll. Can. J. Fish. Aquat. Sci. 41 (10), 1519–1522.
- Stumpf, R.P., 2001. Applications of satellite ocean color sensors for monitoring and predicting harmful algal blooms. J. Hum. Ecol. Risk Assess. 7 (5), 1363–1368.
- Stumpf, R.P., Wynne, T.T., Baker, D.B., Fahnenstiel, G.L., 2012. Interannual variability of cyanobacterial blooms in Lake Erie. PLoS ONE 7 (8), e4244.
- Van der Leeden, F., Troise, F.L., Todd, D.K., 1991. The Water Encyclopedia, second ed. Lewis Publishers, an Imprint of CRC Press, Boca Raton, Florida 880.
- Wang, M.H., Shi, W., 2007. The NIR-SWIR combined atmospheric correction approach for MODIS ocean color data processing. Opt. Express 15 (24), 15722–15733.
- Witter, D.L., Ortiz, J., Palm, S., Heath, R., Budd, J.W., 2009. Assessing the application of SeaWiFS ocean color algorithms to Lake Erie. J. Great Lakes Res. 35 (3), 361–370.
- [www.epa.gov/glnpo/monitoring/sop/index.html](http://www.epa.gov/glnpo/monitoring/sop/index.html).
- [www.Satlantic.com](http://www.Satlantic.com).
- [www.ssi.shimadzu.com/products/products.cfm?subcatlink=tocanalyzers](http://www.ssi.shimadzu.com/products/products.cfm?subcatlink=tocanalyzers).